Construction and Building Materials 201 (2019) 11–32

Contents lists available at ScienceDirect

Construction and Building Materials

journal homepage: www.elsevier.com/locate/conbuildmat

Recycled ceramic waste high strength concrete containing wollastonite particles and micro-silica: A comprehensive experimental study

Seyed Alireza Zareei [a], Farshad Ameri [b,*], Parham Shoaei [c], Nasrollah Bahrami [a]

[a] Department of Civil Engineering, Isfahan (Khorasgan) Branch, Islamic Azad University, Isfahan, Iran
[b] Young Researchers and Elite Club, Isfahan (Khorasgan) Branch, Islamic Azad University, Isfahan, Iran
[c] Department of Civil Engineering, Sharif University of Technology, Tehran, Iran

HIGHLIGHTS

- Workability of HSC mixtures with wollastonite was reduced.
- Improvement in durability properties including water absorption was observed.
- Splitting tensile and flexural strength of HSC with wollastonite were enhanced.
- HSC with ceramic waste aggregate exhibited higher strength at elevated temperatures.

ARTICLE INFO

Article history:
Received 27 September 2018
Received in revised form 8 December 2018
Accepted 21 December 2018

Keywords:
High strength concrete
Wollastonite particles
Recycled waste ceramic aggregate (RWCA)
Micro-silica
Acidic environment
Elevated temperatures
Microstructure

ABSTRACT

This study investigated the effects of combined utilization of wollastonite particles and recycled waste ceramic aggregate (RWCA) on high strength concrete (HSC) properties. Two groups of mixtures were manufactured: 1) concrete mixtures in which cement was partially replaced with wollastonite at values ranging from 10% to 50%, and 2) mixtures in which wollastonite was used at the aforementioned dosages and 50% of natural coarse aggregate was replaced with RWCA. In addition, 10% of cement weight micro-silica was added to all mixtures. The concrete behavior in terms of strength, durability, resistance against acidic environment, and performance under elevated temperatures ranging from 20 °C to 800 °C was assessed. Furthermore, the effect of wollastonite and RWCA inclusions on the microstructure of samples was studies using scanning electron microscopy (SEM). It was shown that wollastonite has an adverse impact on concrete workability and compressive strength. For example, 34% and 6% reduction in slump and 28-day compressive strength at wollastonite dosage of 50% was observed, respectively. On the other hand, the 28-day splitting tensile strength and flexural strength were respectively increased by 4.25% and 10% at 50% wollastonite content with respect to the control concrete. Furthermore, inclusions of RWCA improved the performance of concrete. For example, the 28-day compressive strength was increased by 24% in mixture with 50% wollastonite content with reference to the control concrete. In addition, the strength retention at 800 °C for mixture with RWCA was 16% higher than that of mixture without RWCA. Thus, it was concluded replacing coarse aggregate with RWCA improves the strength and durability properties of concrete and replacing 30% of cement with wollastonite particles strikes a balance between workability and strength of concrete.

1. Introduction

Concrete is one the most widely used structural material in construction industries due to the ease of access of its ingredients, high durability, and low maintenance cost. Large volumes of concrete are being manufactured all around the world, which has raised some concerns regarding depletion of natural raw aggregate [1] and greenhouse effects generated by ordinary Portland cement production [2–5].

In this regard, green concrete construction, which is concerned with effective management of different forms of industrial or agricultural wastes through introducing them into concrete has drawn the attention of many researchers.

In this regard, a great part of the studies has been dedicated to the utilization of industrial by-products such as ground blast

* Corresponding author.
E-mail addresses: a.r.zareei@khuisf.ac.ir (S.A. Zareei), farshadameri@khuisf.ac.ir (F. Ameri).

https://doi.org/10.1016/j.conbuildmat.2018.12.161
0950-0618/

furnace slag [6–9], steel slag [10,11], cement kiln dust [12] and also agricultural by-products including rice husk ash [13], sugarcane bagasse ash [14,15], fly ash [16,17], palm oil fuel ash [18] as replacement of cement or aggregate to manufacture sustainable, green and eco-friendly concrete. Also, other types of materials such as pozzolanic materials [13] and fiber-type materials including metallic fibers [19], polymeric fibers (e.g. nylon and polypropylene) [20], glass fibers [21,22], and natural fibers [23] have been successfully incorporated in concrete production.

With the growth in population and subsequent urban developments, ceramic waste is being disposed in large volumes, causing environmental issues in terms of landfilling and waste treatment. The large amount of this waste material has encouraged many researchers to incorporate it in concrete manufacturing [24,25]. Anderson et al. [26] studied the mechanical behavior of concrete containing 20%, 25%, 35%, 50%, 65%, 75%, 80% and 100% ceramic waste used as replacement of coarse aggregate. Rashid et al. [27] conducted an experimental and numerical study on the performance of concrete with ceramic waste aggregate. It was shown that replacing natural aggregate with 30% ceramic waste leads to the highest compressive strength and minimal environmental impact. Martins et al. [28] evaluated the residual strength of concrete containing 20, 50, and 100% recycled ceramic waste subjected to temperatures of 200, 400, and 600 °C for 60 min. Significant reduction in strength and also spalling were observed at the highest temperature. In a similar study, Vieira et al. [29] studied the behavior of concrete with recycled concrete aggregate used as substitution of natural coarse aggregate at elevated temperatures.

On the other hand, some studies investigated the incorporation of using inert materials such as wollastonite in form of powder or micro-fibers to enhance the microstructure of concrete [16,30,31]. Furthermore, several studies investigated the possibility of using wollastonite in concrete manufacturing. Wahab et al. [32] studied the mechanical properties of mortars in which cement or sand was partially replaced with 10%, 20%, and 30% of wollastonite. According to the results, the compressive and flexural strength were respectively improved by 45% and 28% when 20% of sand was replaced with wollastonite. Dey et al. [33] conducted an experimental study on cementitious composites with wollastonite microfibers and silica fume replaced with cement at 5%, 10%, and 15% values. Results showed that about 30% increase in compressive strength was obtained at 10% replacement level. Kalla et al. [34] studied the durability of concrete incorporating wollastonite particles as replacement of cement by contents varying between 0 and 25%. It was indicated that concrete with 10–15% wollastonite exhibits improved strength and lower porosity.

In the present work, the combined utilization of wollastonite particles and recycled ceramic waste aggregate was studied. According to the available literature, wollastonite particles are effective in improving the tensile and flexural strength of concrete; however, they have an adverse effect on compressive strength. On the other hand, incorporating ceramic waste aggregate in concrete as coarse aggregate enhances its strength. In this regard, this study investigated the possibility of producing a high strength concrete in which high percentages of cement have been replaced with wollastonite particles without compromising its compressive strength. For this purpose, concrete mixtures containing wollastonite particles with replacement ratios of 10–50% by weight of cement were prepared. Furthermore, to evaluate the influence of ceramic waste aggregate on the properties of concrete, another set of mixtures containing the same dosages of wollastonite particles, but with 50% of natural coarse aggregate replaced with ceramic waste aggregate was manufactured. In addition to evaluating the physical, mechanical, and durability properties of concrete mixtures, the effect of elevated temperatures and acidic environment on density and compressive strength of specimens was assessed.

Table 1
Physical properties of wollastonite.

Property	Value
Appearance	White
Shape	Acicular
Dimension (μm)	4–6
Molecular weight	114
Specific gravity	2.91
Specific surface area (m^2/kg)	845
pH	9.9
Water solubility (g/100 cc)	0.0095
Density (kg/m^3)	2899.3
Mohs hardness	4.5
Coefficient of expansion (1/°C)	6.5×10^{-6}
Theoretical melting point (°C)	1540

The outcome of this investigation will provide a comprehensive and practical database for guideline modification, engineering purposes and further investigations on the field of concrete with supplementary materials (Table 1).

2. Experimental program

2.1. Materials

2.1.1. Cement

In this study, cement type II with the 28-day compressive strength of 25 MPa was provided from Shahrekord cement plant. The specific gravity, specific surface area, and density of cement were 3.15, 372.5 m^2/kg, and 3140 kg/m^3, respectively. It is worth mentioning that the specific surface area of cement was calculated by using the Blaine's air permeability technique. The chemical composition of cement is presented in Table 2. In addition, X-ray diffraction (XRD) analysis was carried out on cement particles and the results are demonstrated in Fig. 1. As observed, the abun-

Table 2
Chemical characteristics of cement, micro-silica, and wollastonite used in this study.

Chemical compound	Cement	Micro-silica	Wollastonite
SiO_2	21.68	96.4	48.3
CaO	63.5	0.49	49.8
Al_2O_3	5.9	1.32	0.5
Fe_2O_3	3.2	0.87	0.55
TiO_2	–	–	0.01
MnO	–	–	0.18
MgO	1.8	0.97	0.46
Na_2O	0.2	0.31	0.06
K_2O	0.7	0.21	0.064
SO_3	1.7	0.1	–

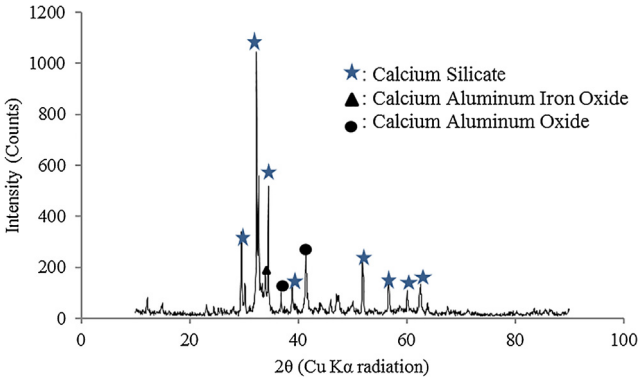

Fig. 1. X-ray diffraction of cement.

dance of calcium silicate (Ca_2SiO_4) and calcium aluminium oxide is evident.

2.1.2. Micro-silica

To enhance the microstructure of concrete mixtures, micro-silica was used at a constant amount of 10% of cement weight in all mixtures. Due to its highly pozzolanic characteristic, it can contribute to the strength gain in concrete mixtures. Micro-silica consists of fine particles with the average size of 0.1–0.2 μm, density of 550–650 kg/m^3, specific surface area of 21000 m^2/kg, and specific gravity of 2.22. The chemical analysis showed that the micro-silica used in this study is composed of 96.4% SiO_2 as tabulated in Table 2, which was in agreement with XRD results where the presence of silicon oxide and quartz was evident as depicted in Fig. 2.

Furthermore, the morphology of MS particles is illustrated in Fig. 3. As observed, they are mostly in angular shape and have a porous structure as shown in Fig. 3(a). In addition, Fig. 3(b) indicates that MS particles have a rough surface.

2.1.3. Wollastonite particles

Basically, the raw wollastonite mainly consists of SiO_2 and CaO. Wollastonite is not categorized as a pozzolanic material; however, it is listed as a hydraulic cement according to Keil-Rankin diagram [35].

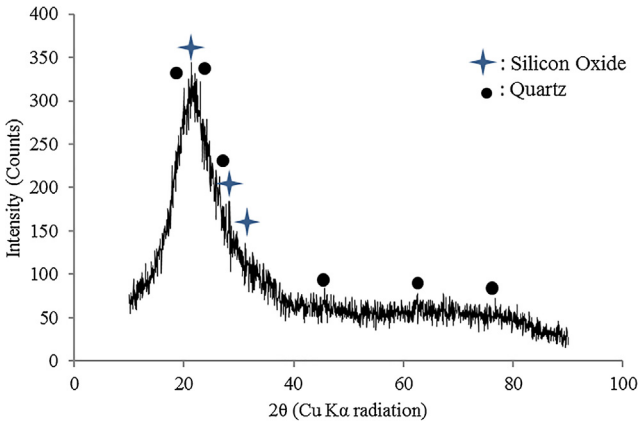

Fig. 2. XRD of micro-silica.

The wollastonite used in this study was produced by Tiva Tejarat Company in Esfahan, Iran. The inorganic wollastonite was reduced in size in two steps by using crushing machines with different sizes and then was grinded by using an air-jet mill to obtain wollastonite with particle size less than 75 μm. Thereafter, the produced wollastonite particles was passed through a sieve with hole diameter of 45 μm using wet sieving technique. It was shown that over 75% of the produced wollastonite passed through the selected sieve. Fig. 4(a) shows the natural inorganic wollastonite (as-received) and Fig. 4(b) shows the wollastonite particle after processing, i.e., in powder form.

Furthermore, the physical properties of wollastonite is tabulated in Table 2. It is worth noting that the specific surface area of wollastonite particles was measured by using Nitrogen adsorption technique.

In addition, grain size distribution of wollastonite was determined by using a LA-960 Laser Particle Size Analyze HORIBA. A comparison between the grain size distribution of cement, micro-silica, and wollastonite is illustrated in Fig. 5. As seen, cement particles were the largest, the next was wollastonite, and micro-silica had the smallest particle size. Also, the chemical properties of the wollastonite together with cement and micro-silica used in the present study are presented in Table 2.

Furthermore, Fig. 6 shows the SEM micrograph of wollastonite particles used in the present study. As observed, the wollastonite particles are amorphous and vary in size and shape (Fig. 6(a)). The angular shape and rough surface of wollastonite particles as shown Fig. 6(d), increases the interlocking between them and the cement paste. Moreover, layered wollastonite particles (Fig. 6(e) and (f)) possess a higher water absorption capacity which consequently, lowers the workability of the resulting mixture. In addition, some wollastonite particles are in the form of micro-fibers as shown in Fig. 6(a)–(c). This important characteristic, results in micro-fiber effect which increases the tensile and flexural strength of concrete through preventing cracks from propagation and further opening as reported by previous studies [33,36,37].

To obtain an understanding about the chemical composition of wollastonite, X-ray diffraction analysis was carried out and the results are illustrated in Fig. 7. As seen, wollastonite particles

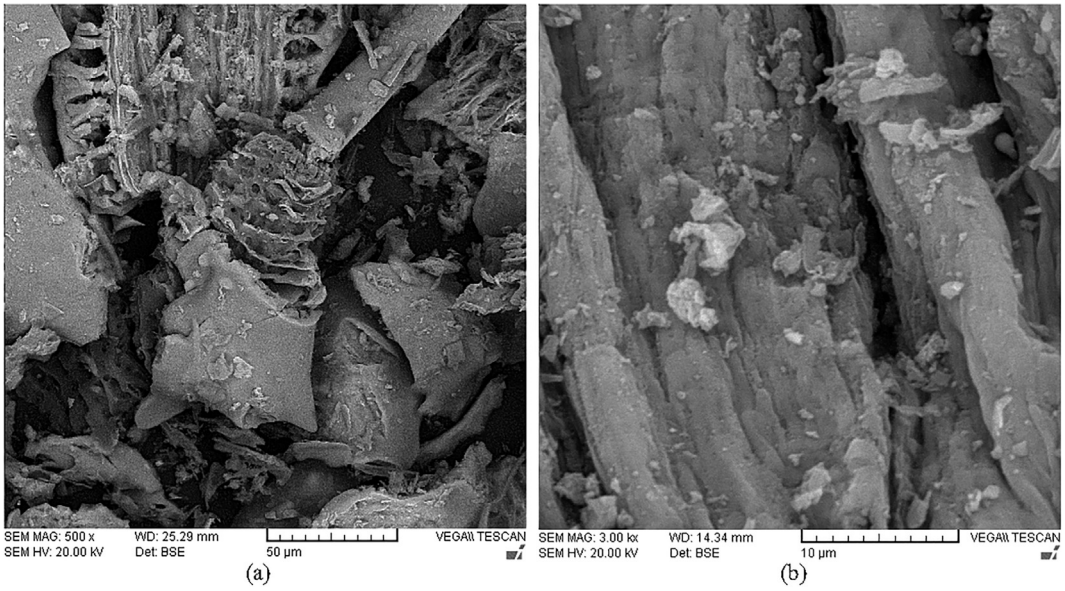

Fig. 3. SEM image of micro-silica particles: (a) 500x magnification, (b) 3000× magnification.

Fig. 4. (a) Natural inorganic wollastonite, (b) Wollastonite in powder form.

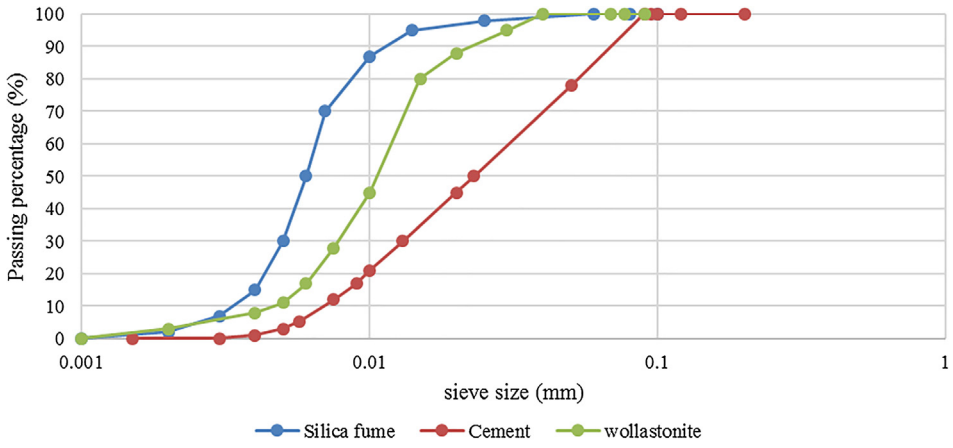

Fig. 5. A comparison between the grain size distribution of cement, micro-silica, and wollastonite.

mainly consist of calcium silicate and olivine, which is a magnesium iron silicate.

2.1.4. Aggregate

Gravel with the particle size varying between 4.75 mm and 19 mm, density of 2250 kg/m^3, and water absorption of 2.65% was used as natural coarse aggregate in this study. Regarding the fine aggregate, washed river sand provided from Sofeh mine with particle size of 0–4.75 mm, density of 2170 kg/m^3, water absorption of 4.6% and fineness modulus of 3.1 was used. Fig. 9 shows the passing percentage of the natural coarse and fine aggregate.

2.1.5. Ceramic waste aggregate

Ceramic waste aggregate was used as partial replacement of coarse aggregate in this investigation. The ceramic wastes were collected from construction sites (Fig. 8(a)) and then they were crushed by using a jaw crusher machine to obtain ceramic aggregate with the particle size of 4.75 mm to 19 mm as shown in Fig. 8(a)–(d). The grain size distribution of ceramic waste aggregate is demonstrated in Fig. 9.

The water absorption of ceramic waste aggregate and natural coarse aggregate was 16.6% and 2.65%, respectively. Furthermore, the density of ceramic waste aggregate was 2461.1 kg/m^3, which is close to that of gravel (2250 kg/m^3); therefore, incorporating them instead of natural coarse aggregate does not influence the weight of the concrete significantly.

Moreover, to obtain an understanding about the mineralogical compounds of the ceramic waste aggregate, X-ray diffraction (XRD) analysis was carried out. As seen in Fig. 10, the predominance of SiO_2 (Quartz) and Zeolite, which mainly consist of silicon and oxygen is clear.

2.2. Concrete mix design

In this study, two groups of concrete mixtures were prepared. In the first group of mixtures, hereinafter referred to as HSCW mixtures, cement was partially replaced with wollastonite particles at 10%, 20%, 30%, 40%, and 50% (by weight of cement) dosages. The second group of mixtures, herein denoted as HSCRW mixtures, were prepared with the same mix proportioning of HSCW mixtures except that 50% of natural coarse aggregate was also replaced with recycled ceramic waste aggregate. All concrete mix designs were determined in accordance with ASTM C192 [38] for a water to binder ratio of 0.38 as presented in Table 3. It should be noted that 10% of cement weight micro-silica was added to all mixtures for the purpose of pore refinement. Furthermore, brown modified polycarboxylic ether (PCE) polymer, with the specific gravity of 1.06 and pH value of 8 was incorporated as super-plasticizer in all mixes with dosage of 2.5% by weight of cementitious materials.

3. Experimental procedures

An extensive experimental program was designed to examine the physical, mechanical, and durability properties of recycled ceramic waste high strength concrete with wollastonite particles. Fresh concrete properties including slump and density were deter-

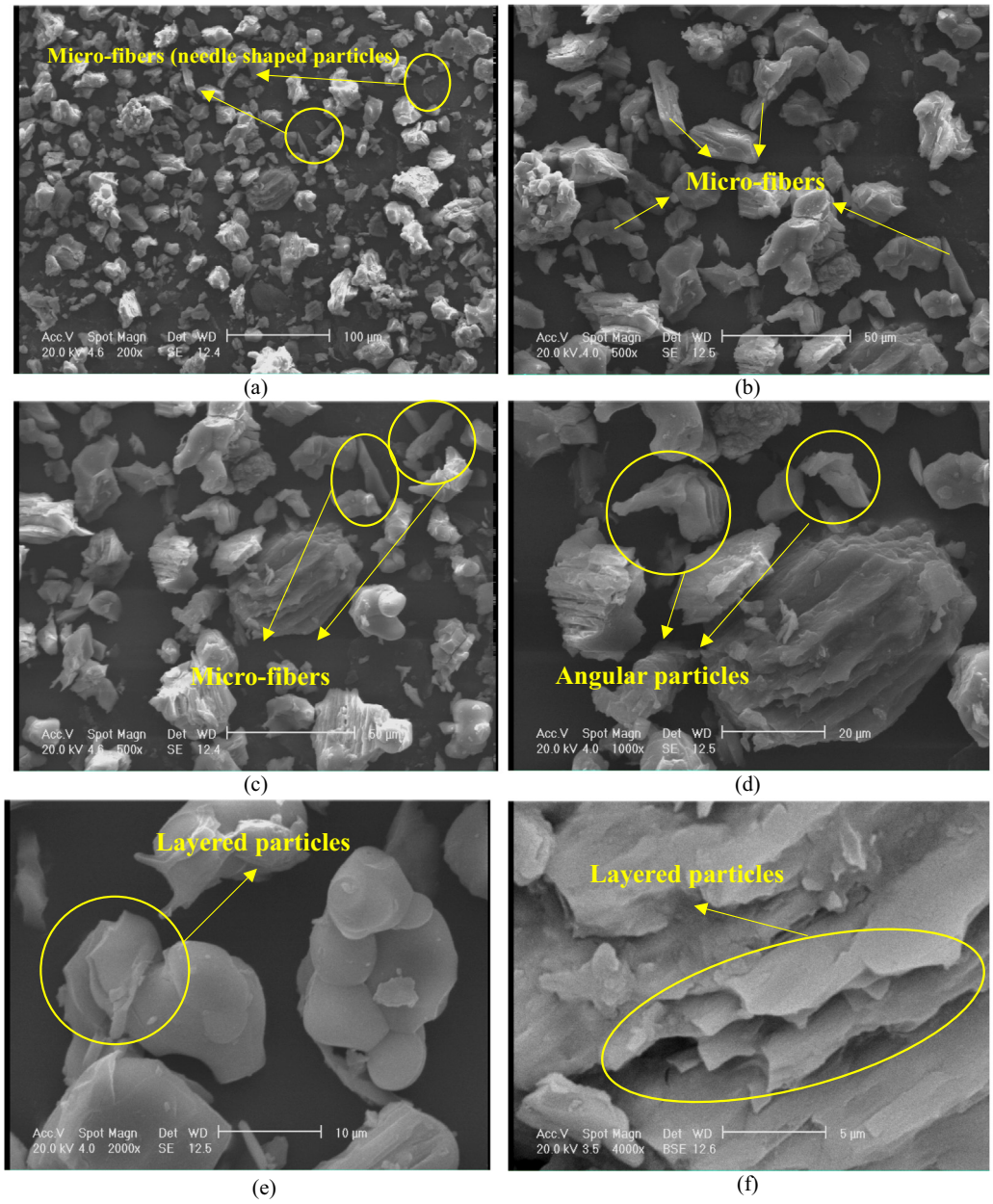

Fig. 6. SEM micrograph of wollastonite particles used in this study: (a) 200× magnification, (b) 500× magnification, (c) 500× magnification, (d) 1000× magnification, (e) 2000× magnification, (f) 4000× magnification.

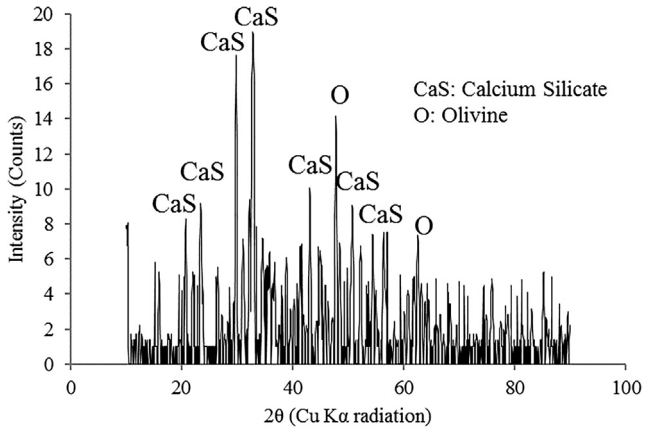

Fig. 7. X-ray diffraction of wollastonite.

mined according to C143/C143M-12 [39] and ASTM C138/C138M-14 [40], respectively. The compressive strength of cubic samples with the side length of 150 mm were determined based on the provisions of ASTM C39/C39M-16 [41]. Note that three specimens were manufactured for each mix design to be tested at the age of 7, 28, and 91 days resulting in 108 specimens. The splitting tensile strength test was conducted on cylindrical samples with the dimensions of 150 mm × 300 mm at the age of 7, 28, and 91 days according to ASTM C496/C496M-17 [42]. Further, the flexural strength of 500 mm × 100 mm × 100 mm beam specimens at curing age of 7, 28, and 91 days was evaluated per ASTM C78/C78M-16 [43]. Note that two specimens were prepared for each mix plan for splitting tensile strength and flexural strength test, i.e., 72 samples were manufactured in total for each test. In addition, the modulus of elasticity test was carried out on 150 mm × 300 mm cylindrical specimens in accordance with ASTM C469/C469M-14 [44].

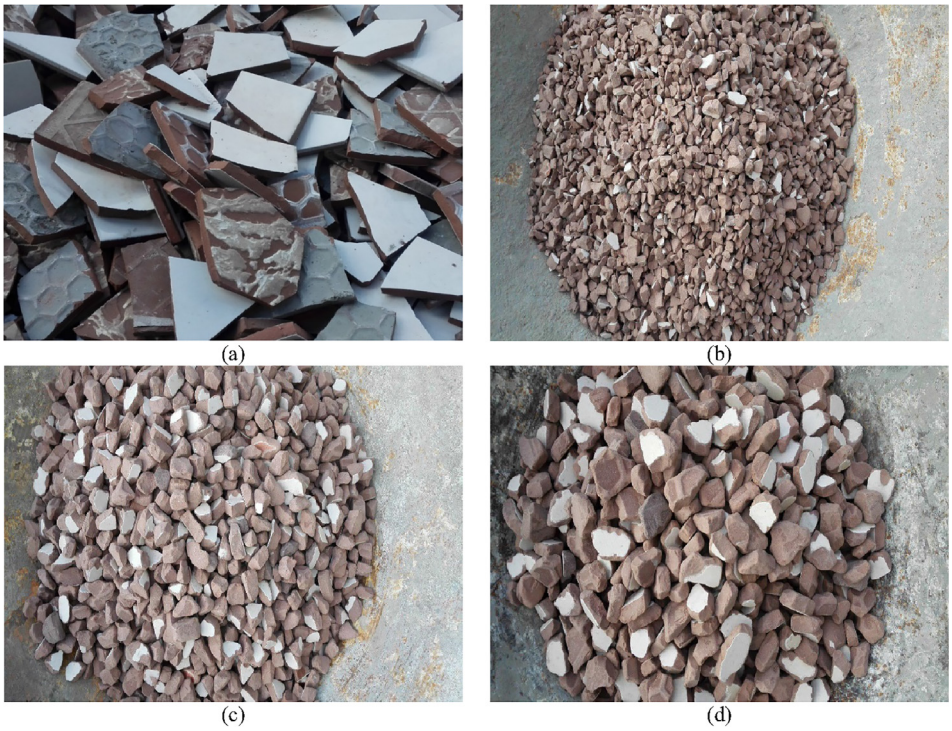

Fig. 8. (a) Waste ceramic collected from construction sites, (b) processed aggregate (4.75–9.5 mm), (c) processed aggregate (9.5–12.5 mm), (d) processed aggregate (12.5–19 mm).

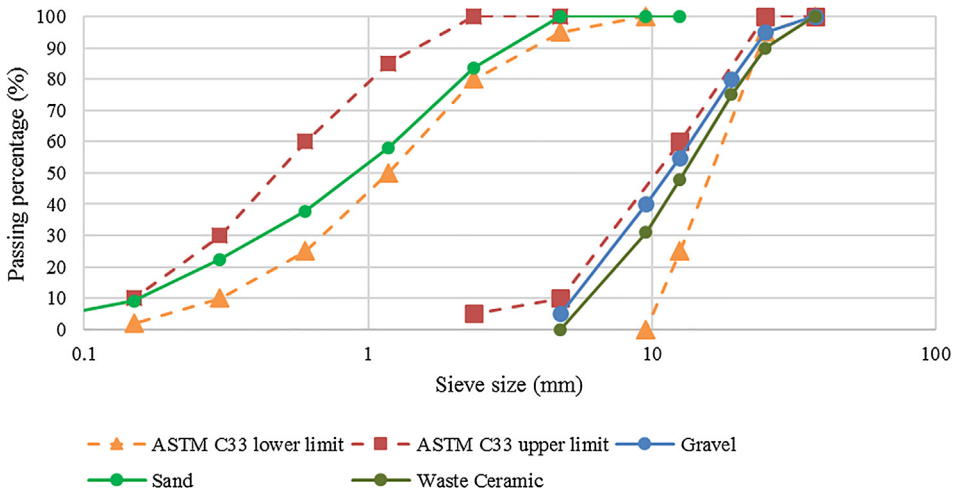

Fig. 9. Grain size distribution.

Moreover, to obtain an insight into the effects of wollastonite particles and recycled ceramic waste aggregate on durability properties of HSC, 24 cubic samples with the side length of 150 mm were immersed in acidic solution with the pH = 2 and their compressive strength and mass variations (per [45]) were determined. Furthermore, the effects of elevated temperatures on density and 28-day compressive strength of cubic samples were studied at temperatures ranging from 25 °C to 800 °C. Also, the water absorption of concrete mixtures was evaluated at the age of 28 days using 100 mm × 100 mm × 100 mm cube samples per [45]. Additionally, the concrete integrity was assessed by using ultrasonic pulse velocity (UPV) test at the age of 28, 56, and 91 days according to ASTM C597 [46]. The specimens were demolded after 24 h and were cured in a water tank at the temperature of 23 °C until the required age.

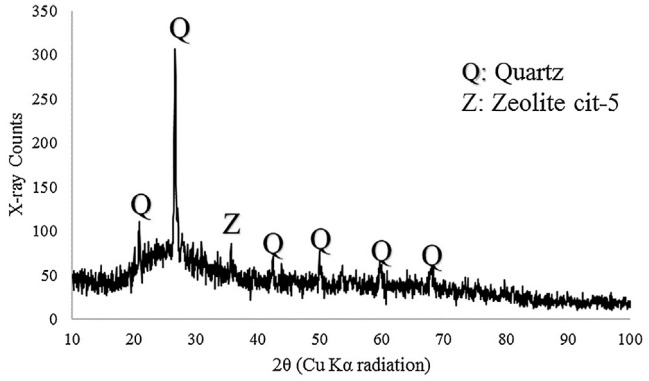

Fig. 10. X-ray diffraction analysis of ceramic waste aggregate.

Table 3
Mix proportioning.

Mix plan	w/b	Cement (kg/m^3)	Water (kg/m^3)	Sand (kg/m^3)	Gravel (kg/m^3)	Wollastonite (%)	Wollastonite (kg/m^3)	Ceramic waste (kg/m^3)	Micro-silica (kg/m^3)	Super-plasticizer (kg/m^3)
HSC[1]	0.38	400	170	700	820	–	–	–	40	10
HSCW[2]10	0.38	360	170	700	820	10	40	–	40	10
HSCW20	0.38	320	170	700	820	20	80	–	40	10
HSCW30	0.38	280	170	700	820	30	120	–	40	10
HSCW40	0.38	240	170	700	820	40	160	–	40	10
HSCW50	0.38	200	170	700	820	50	200	–	40	10
HSCRW[3]0	0.38	400	170	700	410	–	–	410	40	10
HSCRW10	0.38	360	170	700	410	10	40	410	40	10
HSCRW20	0.38	320	170	700	410	20	80	410	40	10
HSCRW30	0.38	280	170	700	410	30	120	410	40	10
HSCRW40	0.38	240	170	700	410	40	160	410	40	10
HSCRW50	0.38	200	170	700	410	50	200	410	40	10

[1] **HSC**: control mix.
[2] **HSCW**: high strength concrete containing wollastonite particles.
[3] **HSCRW**: high strength concrete containing recycled ceramic waste and wollastonite particles.

4. Results and discussion

4.1. Physical properties

4.1.1. Slump

The workability of fresh concrete was measured using slump test. Fig. 11 shows the slump test results for different concrete mixtures. As observed, partial replacement of cement with wollastonite particles caused reduction in slump value of HSCW mixtures. For example, the slump value of HSCW20 and HSCW50

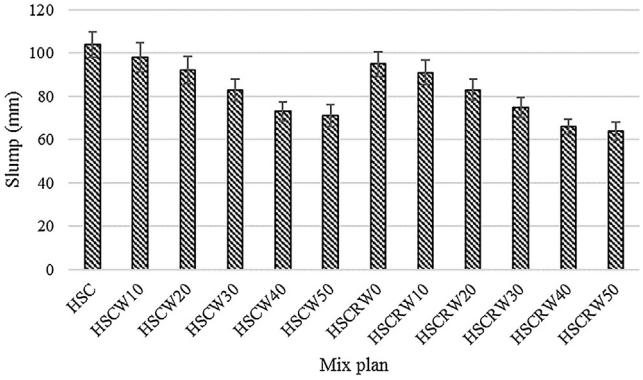

Fig. 11. Slump of concrete mixtures.

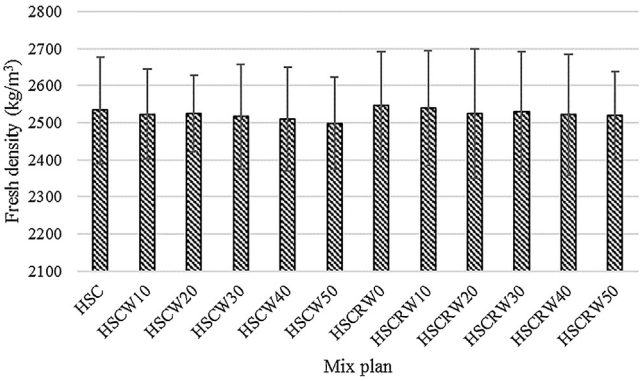

Fig. 12. Fresh density of concrete mixtures.

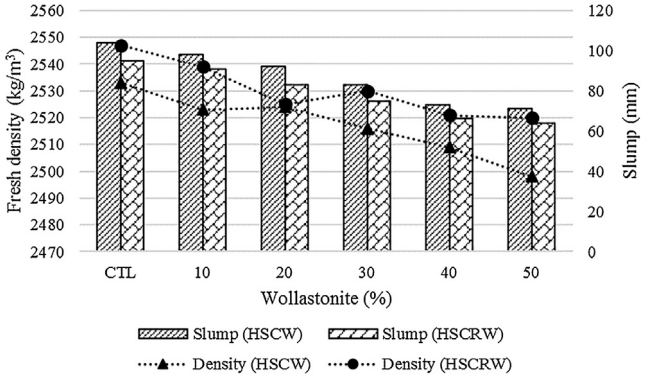

Fig. 13. Variations of fresh concrete density and slump.

Fig. 14. Compression test setup.

was reduced by 15% and 34% as compared to the control concrete, respectively. The reduction was more pronounced when recycled ceramic waste was also included in the mixtures, e.g., 23% and 41% reduction was observed in slump value of HSCRW20 and HSCRW50, respectively. This owed to the fact that wollastonite particles were finer than cement particles, thus they possessed a larger surface area, which increased the water demand of concrete. In addition, recycled ceramic wastes had a higher water absorption capacity compared to the natural coarse aggregate, which resulted in further reduction of workability of concrete.

4.1.2. Fresh density

The fresh concrete density was evaluated based on ASTM C138/C138M-14 [40]. Fig. 12 demonstrates the fresh density of different concrete mixtures. It was observed that the fresh density generally decreased with increasing values of wollastonite and recycled ceramic waste aggregate content; however, its variations was below 1%. The slight reduction in fresh density could be attributed to the fact that the density of wollastonite was relatively lower than that of cement (2.91 g/cm^3 versus 3.15 g/cm^3), which resulted in a lower concrete density. On the other hand, incorporating recycled ceramic waste aggregate led to a minor increase in fresh concrete density owing to the fact that the density of the ceramic waste aggregate used in this study was slightly higher than that of the natural coarse aggregate. For example, the average fresh density of the control concrete was 2533 kg/m^3, while this value for HSCRW0 was 2547 kg/m^3.

The variations of slump and fresh density of concrete is illustrated in Fig. 13. As discussed earlier, with increasing values of wollastonite particles both properties tend to decrease and with inclusions of recycled ceramic waste aggregate, the reduction in slump became more pronounced.

4.2. Mechanical properties

4.2.1. Compressive strength

Compressive strength of concrete is one of the key design factors, which depends on the cement content, water to cement ratio, and aggregate properties. The compressive strength test was conducted on cubic samples at the age of 7, 28, and 91 days per ASTM C39/C39M-16 [41] using a hydraulic jack as shown in Fig. 14.

Fig. 15(a) and (b) respectively show the compressive strength and its variations for concrete mixtures containing wollastonite particles as partial replacement of cement. As observed, the compressive strength tend to decrease with increasing values of wollastonite content; however, the reduction was not considerable. For example, the compressive strength of HSCW50 was reduced by 6% as compared to the control sample. The reduction in strength could be attributed to the fact that the amount of CSH gel produced due to hydration, decreased as cement was replaced with wollastonite particles. This reduction in CSH gel could not be offset by

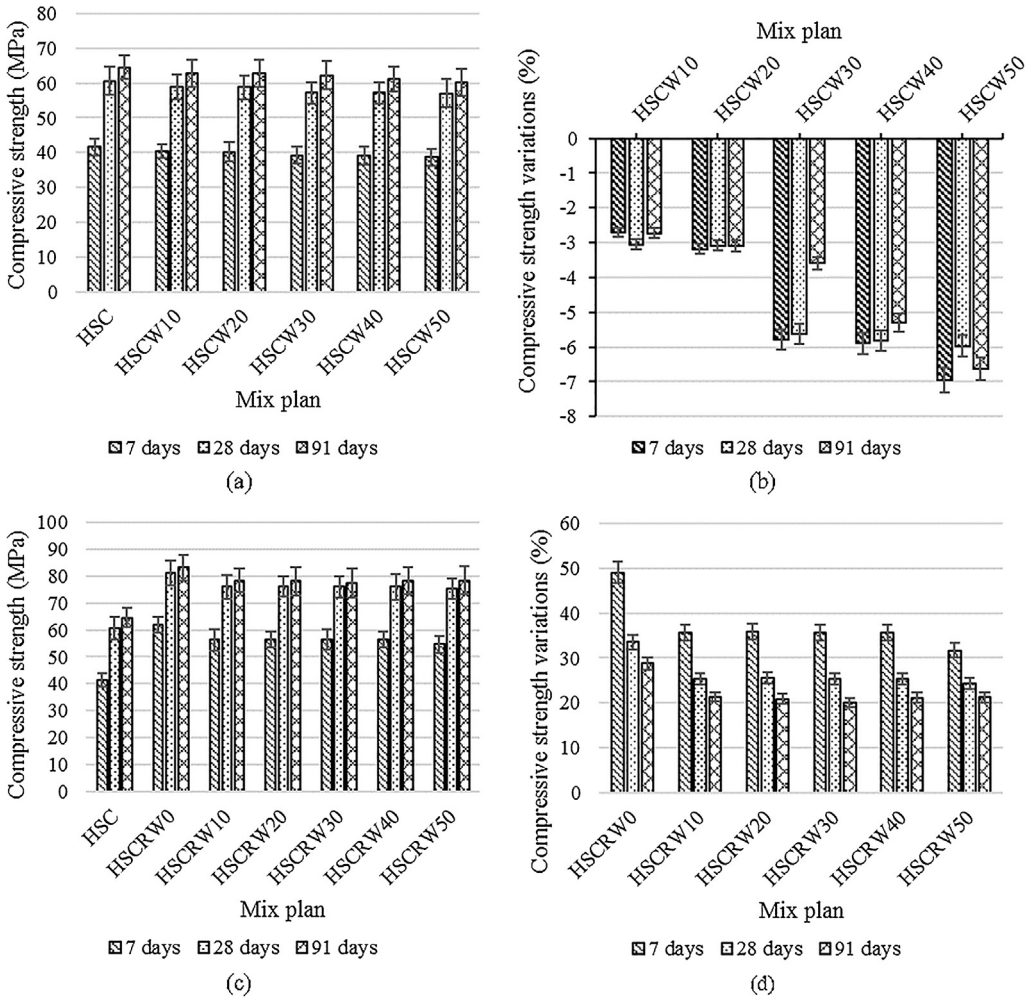

Fig. 15. Compressive strength of concrete mixtures: (a) Compressive strength of HSCW mixtures, (b) Compressive strength variations of HSCW mixtures with respect to HSC, (c) Compressive strength of HSCRW mixtures, (d) Compressive strength variations of HSCRW mixtures with respect to HSC.

micro-filling effect of these particles [32] and as a result, wollastonite did not contribute to the strength development and weakened the bond between concrete components as its content increased. The results were in agreement with findings of other studies. Kalla et al. [16] reported that the compressive strength of concrete in which cement was partially replaced with wollastonite and fly ash declined from 37.53 MPa to 34.1 MPa when wollastonite content was increased from 10% to 25%. Also, Abdel Wahab et al. [32] investigated the properties of mortars containing wollastonite particles as partial replacement of cement. It was shown that replacing 30% of cement with wollastonite particles resulted in 35% reduction in compressive strength.

Furthermore, as seen in Fig. 15(c) and Fig. 15(d), incorporation of ceramic waste aggregate as partial replacement of natural coarse aggregate led to a significant improvement in the compressive strength. The highest compressive strength was recorded for HSCRW0 in which the 7-, 28-, and 91-day compressive strength was increased by 50%, 34%, and 29% with reference to the control sample, respectively. Based on the experiments results, the strength gain was more pronounced at earlier ages due to the pozzolanic activity of ceramic wastes, which contributed to the strength gain during hydration process. Furthermore, the angular shape and rough surface of ceramic waste aggregate increased the interlocking and bond between aggregate and cement paste. The results were comparable with earlier findings. Rashid et al. [27] noticed that the compressive strength of concrete containing 30% ceramic waste aggregate as partial replacement of coarse aggregate was increased by 30%. This increase was attributed to addition of more pozzolanic material. In addition, the rough surface of the ceramic waste aggregate provided physical anchorage while its higher porosity compared to the natural coarse aggregate increased the anchorage between hydrated products and aggregate (chemical anchorage). Medina et al. [47] showed that replacing 25% of the natural coarse aggregate with ceramic waste aggregate increased the compressive strength by 11% as compared to the concrete, which was attributed to the improvements in the interfacial transition zone between ceramic waste aggregate and paste. In another study, Medina et al. [48] stated that using ceramic waste aggregate with grain size greater than 4 mm gave rise to hydrated products such as calcium silicate hydrate or calcium aluminate hydrate due to its sufficient pozzolanic activity which facilitated the reaction with portlandite present in the vicinity of aggregate. Higashiyama et al. [49] also reported that the 28-day compressive strength of the mortar in which 60% of fine aggregate was partially replaced with ceramic waste aggregate increased from 51.6 MPa to 67.4 MPa. It was concluded that the pozzolanic reactivity of ceramic powder was responsible for the increase in strength.

4.2.2. Splitting tensile strength

The splitting tensile strength of cylindrical specimens with the dimensions of 15 cm × 30 cm were evaluated at different curing

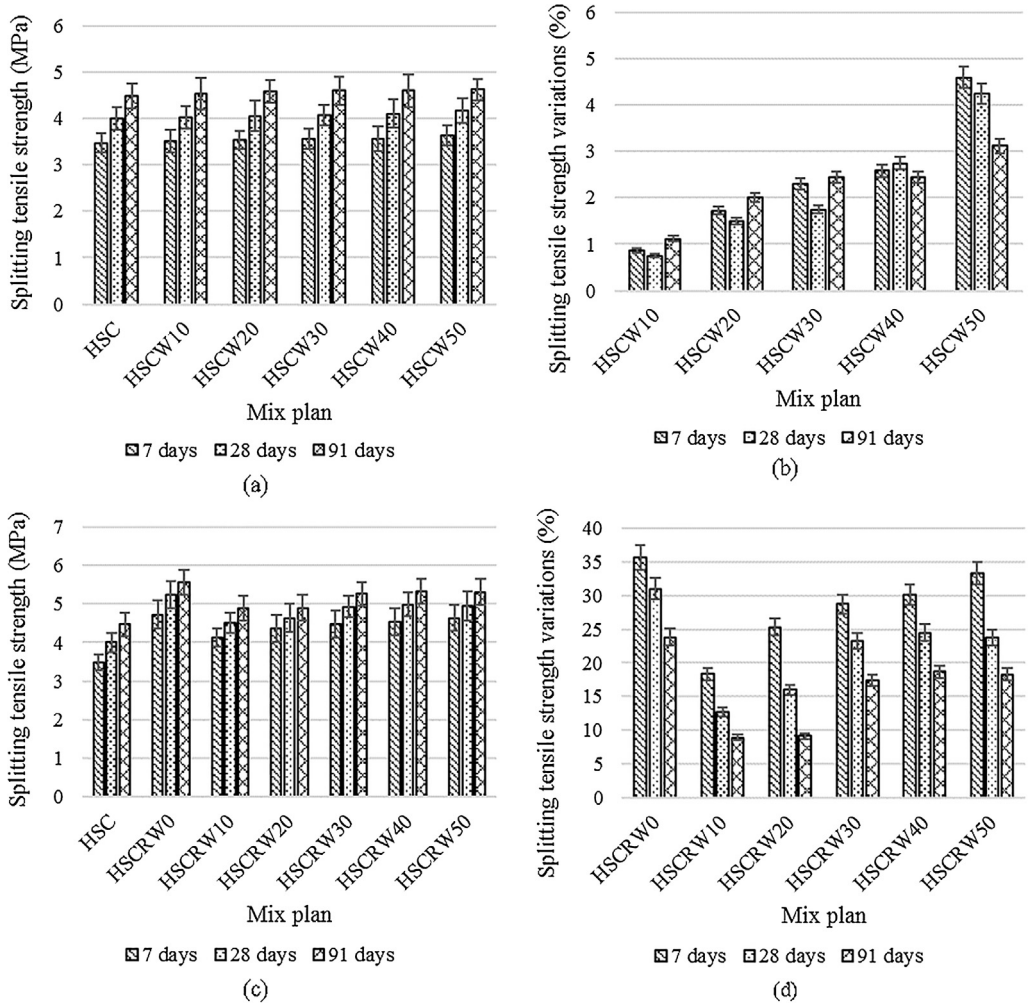

Fig. 16. Splitting tensile strength: (a) Splitting tensile strength of HSCW mixtures, (b) Splitting tensile strength variations of HSCW mixtures with respect to HSC, (c) Splitting tensile strength of HSCRW mixtures, (d) Splitting tensile strength variations of HSCRW mixtures with respect to HSC.

ages. The splitting tensile strength, T, of a specimen with the length l and diameter d is calculated as follows [42]:

$$T = 2P/\pi ld \quad (1)$$

where P refers to the maximum applied load. Fig. 16 shows the splitting tensile strength of different concrete mixtures at different ages. As observed, partial replacement of cement with wollastonite particles slightly improved the tensile strength of concrete. As seen in Fig. 16(a) and (b), the splitting tensile strength demonstrated an increasing trend with increasing values of wollastonite content. For example, about 5% improvement was observed in 28-day tensile strength of concrete containing 50% wollastonite. This slight increase could be related to the high modulus of wollastonite as reported by Mathur et al. [50] and fibrous nature of wollastonite particles, which arrested cracks and prevent them from further opening [32]. Furthermore, the increase in strength was more pronounced in concrete mixtures with wollastonite particles and recycled ceramic waste aggregate. With reference to Fig. 16(c) and (d), about 16% and 24% increase in 28-day splitting tensile strength of HSCRW20 and HSCRW50 were observed compared to the control sample, respectively. The strength gain owed to the pozzolanic characteristic of the recycled ceramic waste aggregate in addition to its rough surface and higher porosity compared to the natural coarse aggregate increased the anchorage between hydrated products and aggregate. In addition, it was observed that the strength development at earlier ages was more pronounced. For example, 33%, 24%, and 18% increase in tensile strength of HSCRW50 were observed compared to the plain concrete at the ages of 7 days, 28 days, and 91 days, respectively.

4.2.3. Flexural strength

Three-point flexural test was conducted on beam specimens at the ages of 7 days, 28 days, and 91 days per ASTM C78/C78M-16 [43]. The test results are depicted in Fig. 17. As seen in Fig. 17(a) and (b), flexural strength of concrete mixtures with wollastonite particles generally increased, e.g., about 10% increase in 28-day flexural strength of HSCW50 was observed. Similar to the splitting tensile strength, the increase in the flexural strength could be ascribed to the filling effect of wollastonite particles, which reduced the void spaces in the concrete matrix and also their needle shape which enable them to bridge between two sides of a crack and inhibit further propagation. Furthermore, inclusions of recycled ceramic waste aggregate contributed to the flexural strength of specimens according to Fig. 17(c) and (d). For example, the 28-day flexural strength of HSCRW0 increased from 5.75 MPa to 6.41 MPa (11.5% improvement). The flexural test results also confirmed the fact that higher strength gain occurred at earlier ages. For example, approximately 16%, 9%, and 5% increase in the flexural strength of mix HSCRW50 were observed at the age of 7 days, 28 days and 91 days, respectively.

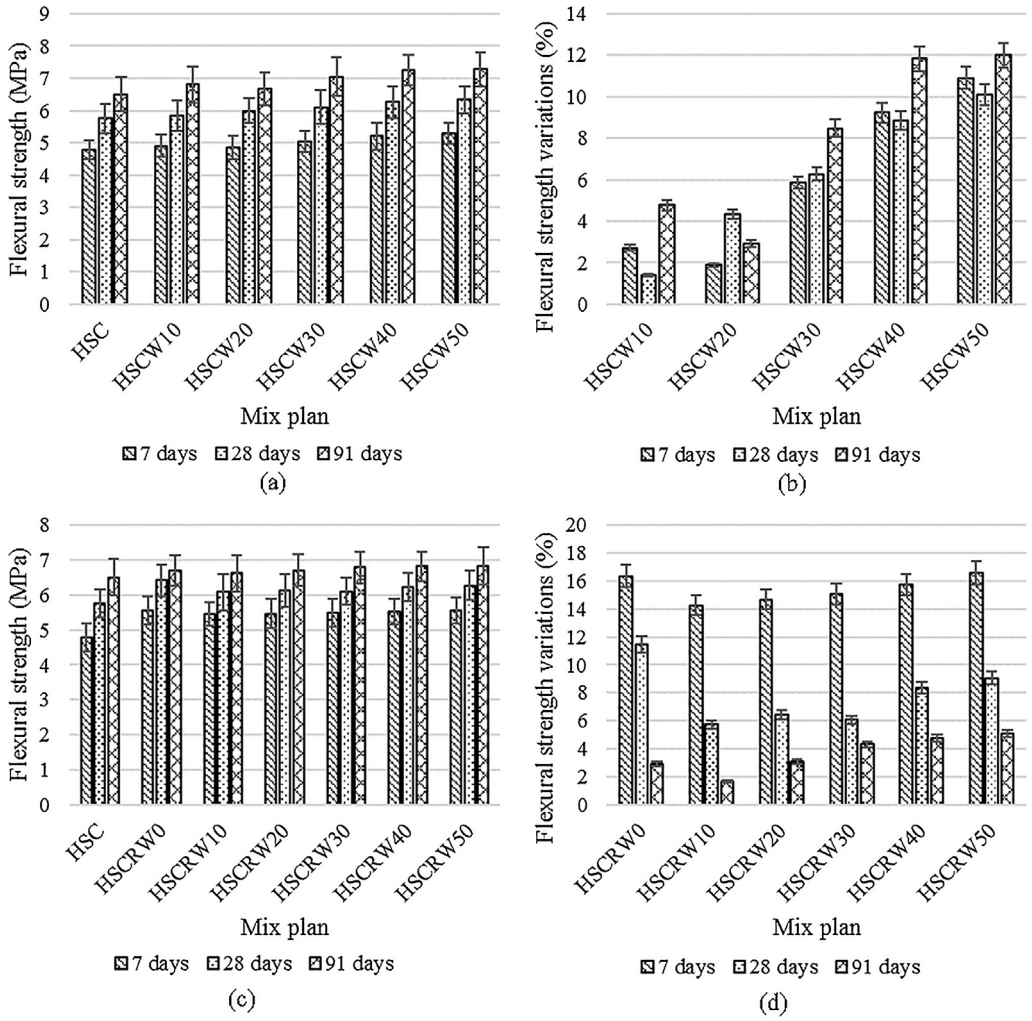

Fig. 17. Flexural strength of concrete mixtures: (a) Flexural strength of HSCW mixtures, (b) Flexural strength variations of HSCW mixtures with respect to HSC, (c) Flexural strength of HSCRW mixtures, (d) Flexural strength variations of HSCRW mixtures with respect to HSC.

4.2.4. Modulus of elasticity

The modulus of elasticity of cylindrical samples was evaluated after 28 days of curing. Fig. 18 shows the modulus of elasticity of concrete mixtures and its variations. As observed, with increasing values of wollastonite content, a slight reduction occurred in the modulus of elasticity. For example, the modulus of elasticity decreased from 38.9 GPa to 37.74 GPa in HSCW50, i.e., approximately 3% reduction occurred.

On the other hand, replacing natural coarse aggregate with recycled ceramic waste aggregate improved the modulus of elasticity of concrete mixtures. For the sake of illustration, replacing 50% of gravel with ceramic waste aggregate led to 9% increase in the modulus of elasticity of HSCRW0 compared to the control concrete HSC.

Although combined utilization of wollastonite particles and recycled ceramic waste had a positive influence on modulus of elasticity of concrete mixtures compared to the plain concrete, with increasing wollastonite content in HSCRW mixtures, the modulus of elasticity demonstrated a decreasing trend. For example, about 4% reduction was observed in the modulus of elasticity of HSCRW50 compared to HSCRW0.

4.2.5. Linear regression analysis

In this section, the correlation between different mechanical properties was investigated. As seen in Fig. 19, a direct correlation exists between the mechanical properties and the compressive strength. Furthermore, a linear regression analysis was carried out to find relationships between the mechanical properties. The results of the linear regression analyses are presented in Table 4 in the form of predictive equations. In this table, f_c is the compressive strength, f_{st} denotes the splitting tensile strength, f_r represents flexural strength, and E_c refers to the modulus of elasticity of the concrete. The equations presented in Table 4 were calibrated against the experimental data and according to the linear regression analysis results, the accuracy of the derived equations was acceptable and they could be used to predict the mechanical properties based on the compressive strength of the concrete.

4.2.6. Comparison between experimental results and design code expressions

In this section, the equations proposed by the existing deign codes which are provided in Table 5, were used to estimate the mechanical properties of concrete including the elastic modulus E_c, flexural strength (f_r), and splitting tensile strength (f_{st}) with respect to the compressive strength (f_c) or characteristic compressive strength (f_{cm}). Furthermore, the predicted values were compared with the experimental results in order to investigate the applicability of design code expressions to HSCW and HSCRW concretes.

A comparison between the mechanical properties obtained by experiment and design codes are depicted in Fig. 20 to Fig. 22. Regarding the modulus of elasticity of HSCW mixtures, EC-04 [53] and JCI-08 [55] provided the closest estimation to the experimental modulus of elasticity; whereas, NZS 3101 [56] and ABA [57]

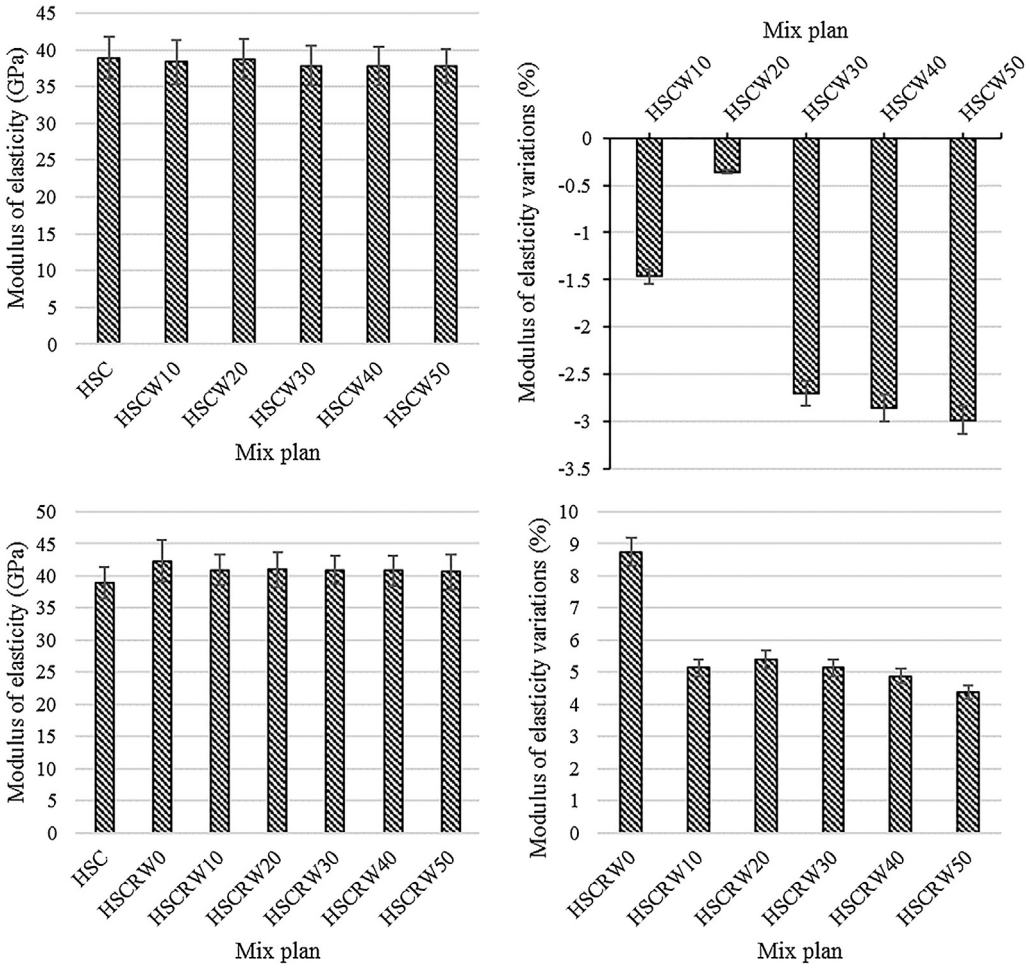

Fig. 18. Modulus of elasticity of concrete mixtures: (a) Modulus of elasticity of HSCW mixtures, (b) Modulus of elasticity variations of HSCW mixtures with respect to HSC, (c) Modulus of elasticity of HSCRW mixtures, (d) Modulus of elasticity variations of HSCRW mixtures with respect to HSC.

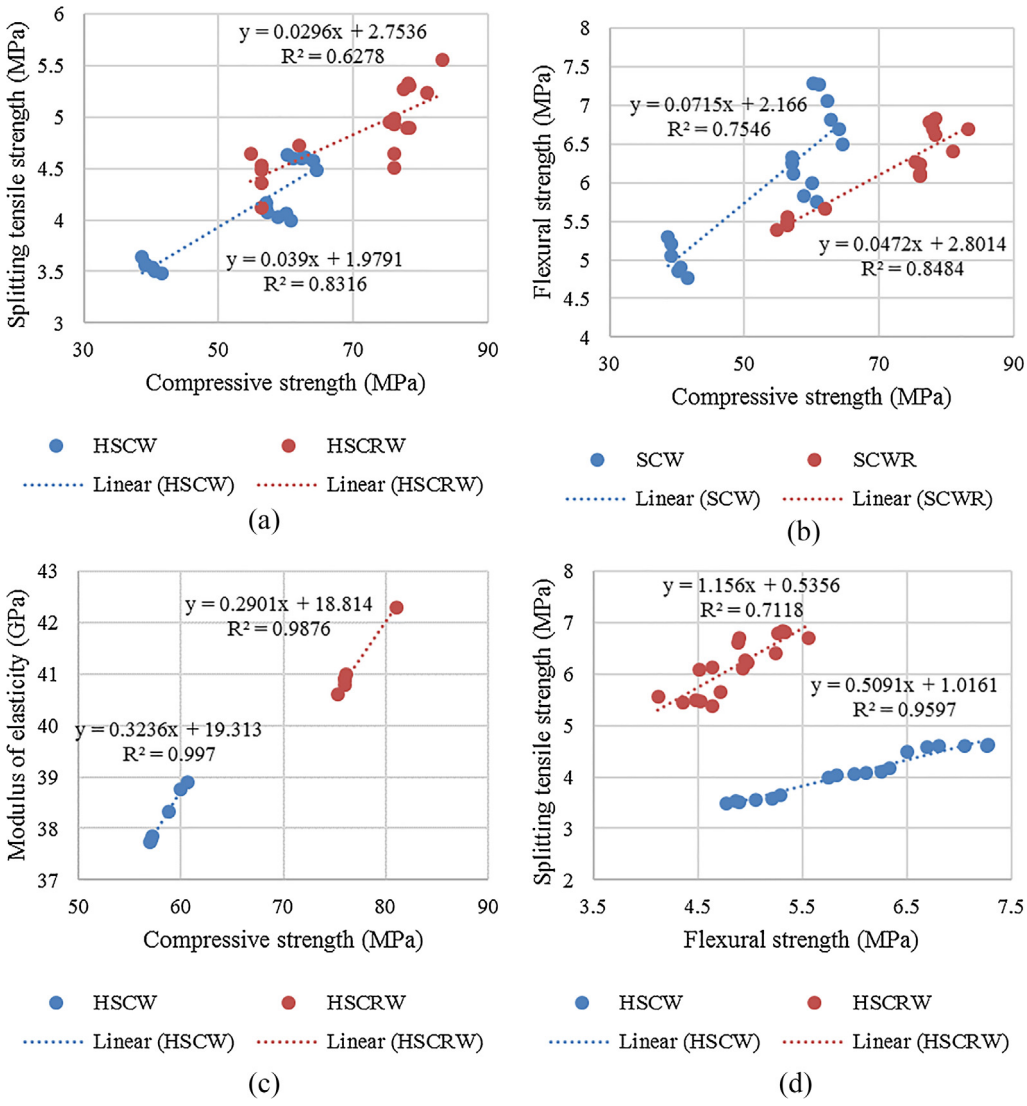

Fig. 19. (a) Relationship between f_{st} and f_c, (b) Relationship between f_r and f_c, (c) Relationship between E_c and f_c, (d) Relationship between f_{st} and f_r.

Table 4
Derived relationships between different properties.

HSCW	R^2	Eq. #	HSCRW	R^2	Eq. #
$f_{st} = 0.039f_c + 1.9791$	0.83	2	$f_{st} = 0.0296f_c + 2.7536$	0.63	3
$f_r = 0.0715f_c + 2.166$	0.75	4	$f_r = 0.0472f_c + 2.8014$	0.85	5
$E_c = 0.3236f_c + 19.313$	0.99	6	$E_c = 0.2901f_c + 18.814$	0.99	7
$f_{st} = 0.5091f_r + 1.0161$	0.96	8	$f_{st} = 1.156f_r + 0.5356$	0.71	9

underestimated the modulus of elasticity. For HSCRW concrete mixtures, the modulus of elasticity estimated by ACI 318-14 [51], EC-04 [53] and JSCE-07 [54] was close to that of the experiment. Similarly, NZS 3101 [56] and ABA [57] underestimated the modulus of elasticity, but JCI-08 [55] provided overestimated values.

Furthermore, Fig. 21 presents the splitting tensile strength values for HSCW and HSCRW concrete mixtures. Based on the results, the values predicted by ACI 318-14 [51] and JCI-08 [55] were the closest, while JSCE-07 [54] and NZS 3101 [56] underestimated the splitting tensile strength for both HSCW and HSCRW mixtures. Further, the values estimated by EC-04 [53] were approximately 14% (by average) higher than the corresponding experimental values.

The flexural strength of HSCW and HSCRW mixtures are illustrated in Fig. 22. As observed, all design codes except EC-04 [53], underestimated the flexural strength in HSCW mixtures by 20% (by average). On the other hand, EC-04 [53] overestimated the flexural strength approximately by 10%. A similar trend was observed for HSCRW mixtures; however, the difference between EC-04 [53] and experiment was more pronounced and the flexural strength was overestimated by 30%.

4.3. Durability properties

4.3.1. Water absorption

Water absorption of cubic specimens with the side length of 10 cm was evaluated per [45]. The water absorption is determined as below:

$$W_i = 100 \times \frac{W_w - W_D}{W_D} \quad (2)$$

where W_i is the water absorption at 30 min, W_D refers to the dried specimen's weight (heated in oven for 72 h), and W_w denotes the specimen's weight after immersion in water for 30 min. Fig. 23 demonstrates the variation of water absorption together with slump for different concrete mixtures. As observed, increasing the wollastonite content in HSCW mixtures resulted in a decrease in the water absorption. For example, 19% and 33% decrease was observed in water absorption of HSCW30 and HSCW50 compared to the control sample. Furthermore, a similar behavior was observed for concrete mixtures in which 50% of natural coarse aggregate was partially replaced with ceramic waste aggregate.

Table 5
Equations proposed by design codes.

Standard	Modulus of elasticity (E_c) (GPa)	Flexural strength (f_r) (MPa)	Splitting tensile strength (f_{st}) (MPa)
ABA (Iran)	$E_c = 5\sqrt{f'_c}$	$f_r = 0.60\sqrt{f'_c}$	–
ACI 318-14 [51]	$E_c = 4.73\sqrt{f'_c}$	$f_r = 0.62\sqrt{f'_c}$	$f_{st} = 0.53\sqrt{f'_c}$
CSAA23.3-04 [52]	$E_c = 4.5\sqrt{f'_c}$	$f_r = 0.60\sqrt{f'_c}$	–
EC-04 [53]	$E_c = 22\left(\frac{f_{cm}}{10}\right)^{0.3}$	$f_r = 0.435 f_c'^{2/3}$	$f_{st} = 0.3 f_c'^{2/3}$
JSCE-07 [54]	$E_c = 4.7\sqrt{f'_c}$	–	$f_{st} = 0.44\sqrt{f'_c}$
JCI-08 [55]	$E_c = 6.3 f_c'^{0.45}$	–	$f_{st} = 0.13 f_c'^{0.85}$
NZS 3101 [56]	$E_c = 3.32\sqrt{f'_c} + 6.9$	$f_r = 0.60\sqrt{f'_c}$	$f_{st} = 0.44\sqrt{f'_c}$

f_c and f_{cm} are the mean compressive strength and the mean characteristic compressive strength of concrete, $f_c = f_{cm} - 8$ per EC – 04 [53].

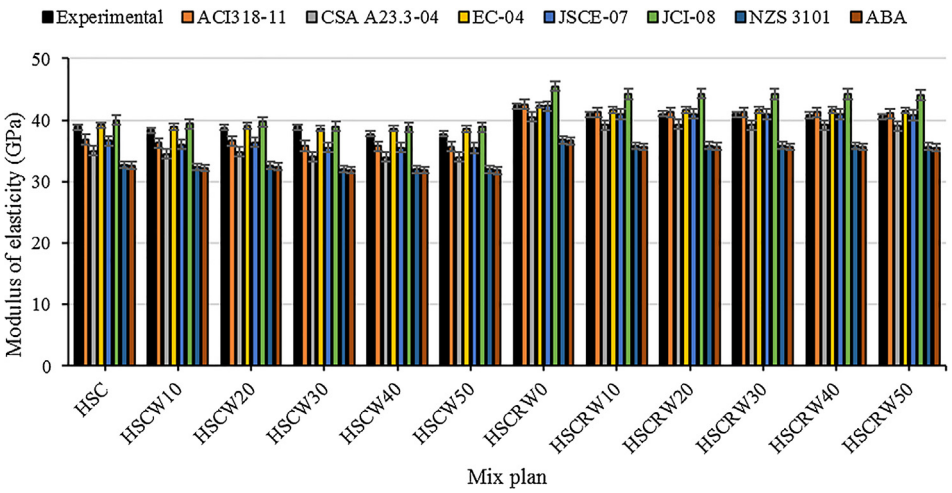

Fig. 20. Comparison between the modulus of elasticity of concrete mixtures obtained by experiment and design codes.

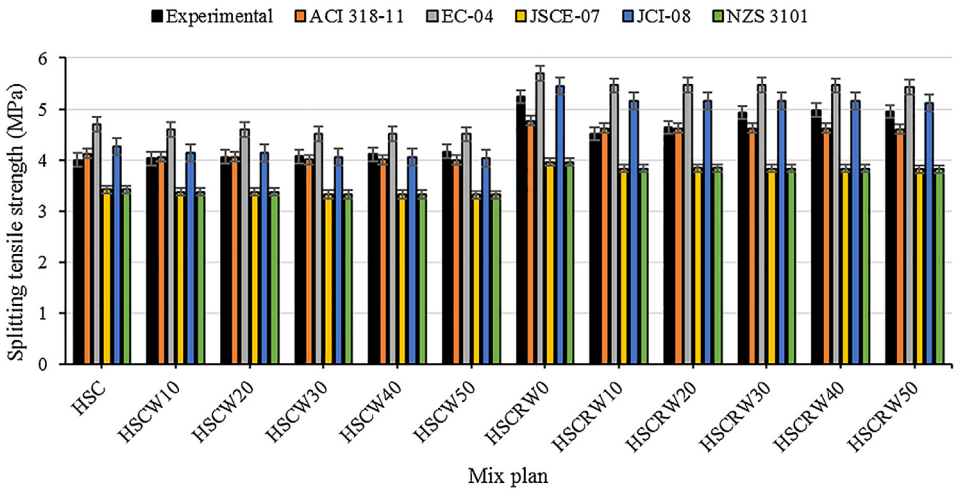

Fig. 21. Comparison between the splitting tensile strength of concrete mixtures obtained by experiment and design codes.

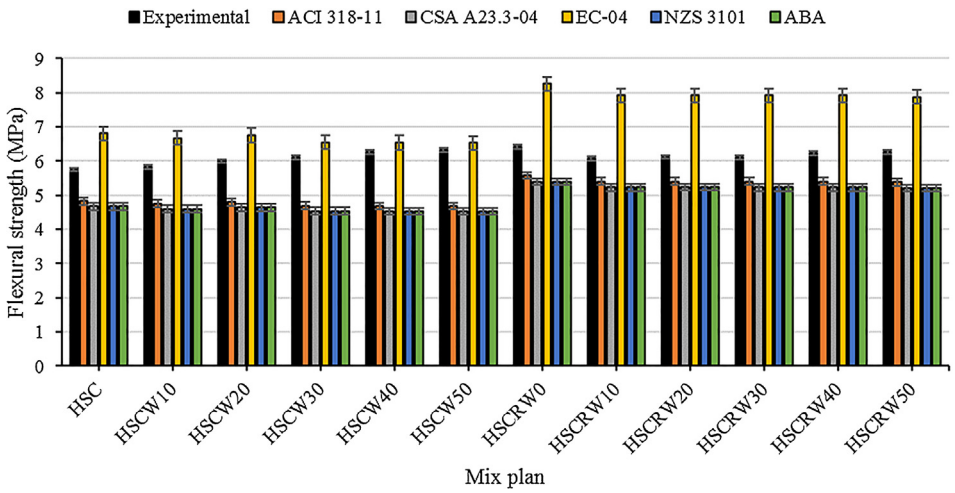

Fig. 22. Comparison between the flexural strength of concrete mixtures obtained by experiment and design codes.

For the sake of illustration, the water absorption of HSCRW10, HSCRW20, and HSCRW30 were 2.26%, 2.11%, and 1.98%, i.e., 9%, 15%, and 20% reduction was observed compared to the plain concrete. This owed to the fact that the wollastonite particles filled the pores and voids in the concrete texture and produced a denser matrix, which in turn reduced the water absorption of the concrete. This supports the findings of other researchers that reported the inclusions of wollastonite particles reduced the water permeability and water absorption of concrete and improved its durability [16,34,58]. Ransinchung et al. [58] reported that concrete with 15% wollastonite used as substitution of cement exhibited reduced water absorption up to 30% with respect to (w.r.t) control mix.

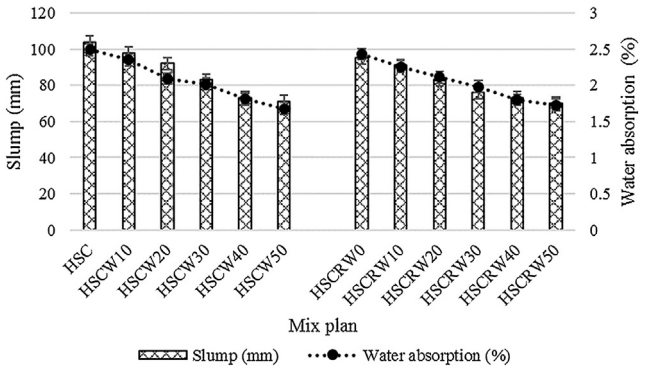

Fig. 23. Variation of water absorption versus slump.

4.3.2. Effects of exposure to acidic environment on concrete properties

This section briefly summarizes the effects of exposure to acidic environments on physical and strength properties of concrete specimens containing wollastonite particles and ceramic waste aggregate. For this purpose, three cubic samples with the side length of 15 cm were manufactured for each mixture and they were cured in a water tank for 28 days. Thereafter, the control samples were kept in the water tank for another 28 days, while the other specimens were immersed in a 5% sulfuric acid (H_2SO_4) solution with pH = 2, molar mass of 98.08 g/mol, and density of 1.84 g/cm^3 for the same period of time. Meanwhile, the pH of the solution was controlled by using a pH meter device. Fig. 24 compares the unconditioned and conditioned specimens regarding their physical appearance. The effects of acidic environment on concrete properties including mass and compressive strength were investigated and the results are presented in the following sections.

4.3.2.1. Mass variations. The specimens were precisely weighted before and after exposure to the acidic environment to determine the mass variations due to corrosion. Fig. 25(a) and (b) illustrate

Fig. 24. (a) Unconditioned specimens, (b) Conditioned specimens after 28 days immersion in acidic solution.

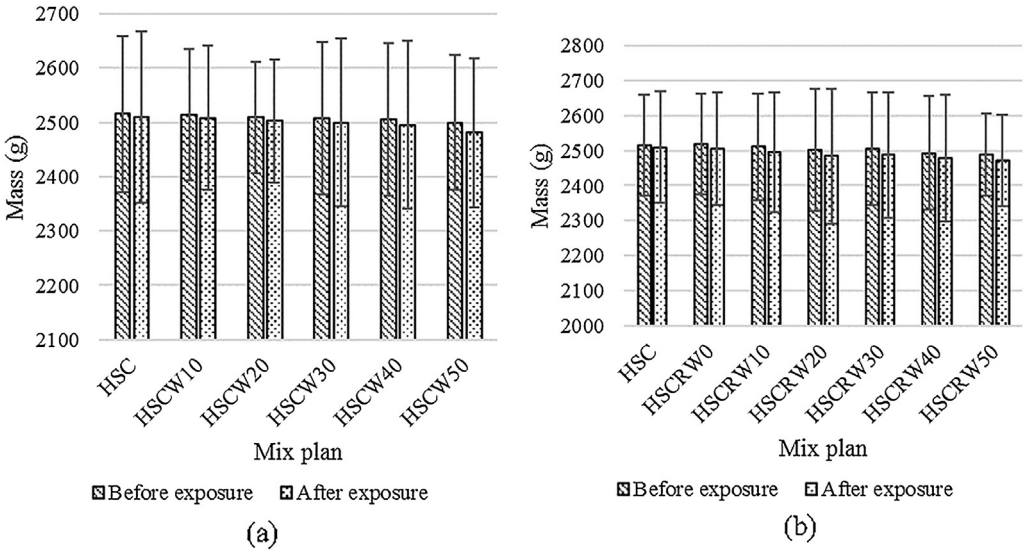

Fig. 25. Mass of concrete specimens: (a) Mass of HSCW mixtures, (b) Mass of HSCRW mixtures.

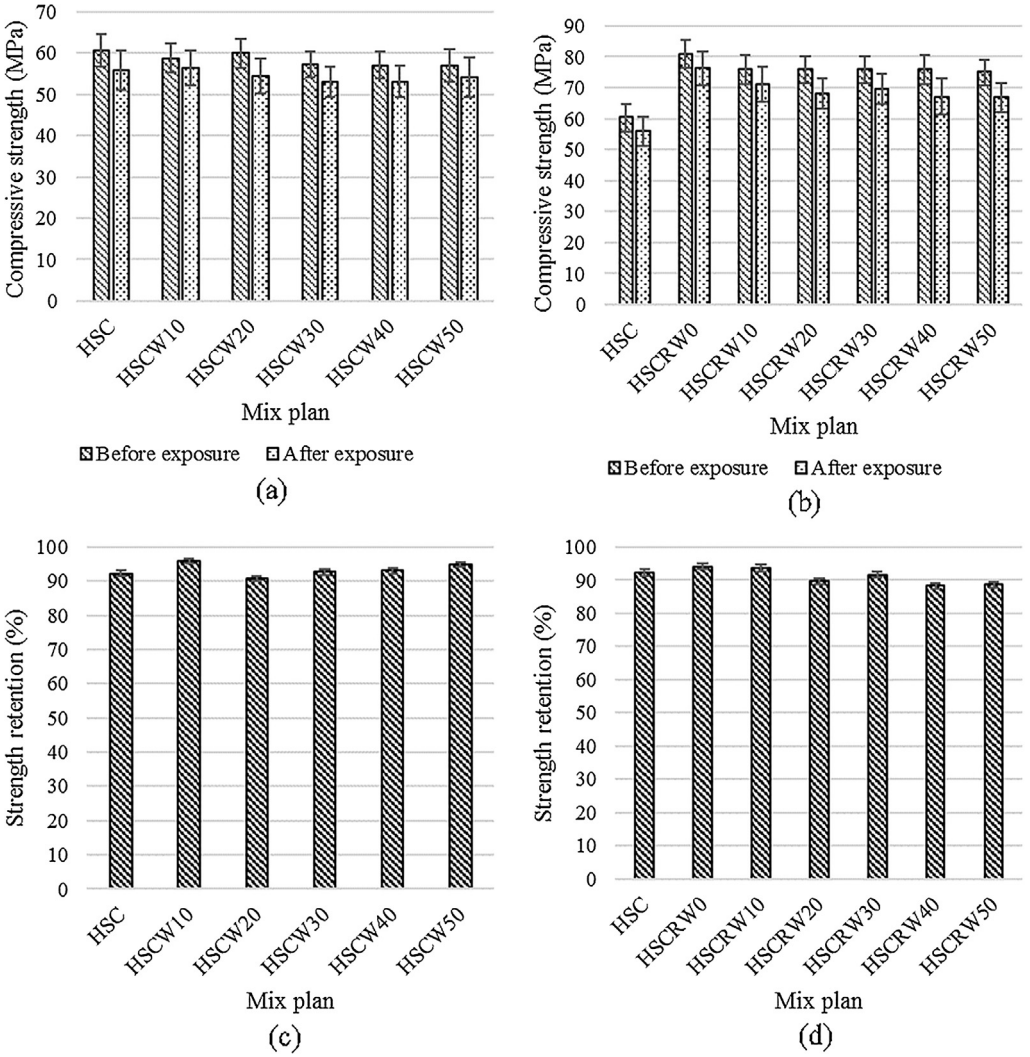

Fig. 26. (a) Compressive strength of HSCW mixtures, (b) Compressive strength of HSCRW mixtures, (c) Strength retention of HSCW mixtures after exposure to acidic solution, (d) Strength retention of HSCRW mixtures after exposure to acidic solution.

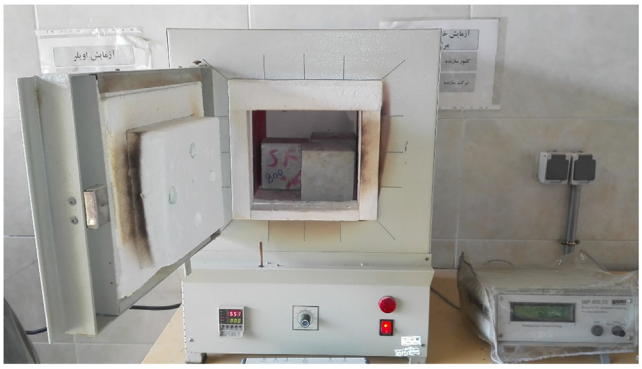

Fig. 27. Electric oven.

the mass variation of HSCW and HSCRW concrete mixtures, respectively. As observed, with increasing values of wollastonite content, the mass of the samples decreased; however, the reduction percentage was below 1%. For example, 0.4% and 0.75% reductions were observed in HSCW40 and HSCW50 compared to the control sample, respectively. Furthermore, the mass variations were more pronounced in HSCRW mixtures in which 50% of natural coarse aggregate was replaced with ceramic waste aggregate. For example, the sample's mass decreased by 0.6% and 0.76% respectively for HSCRW40 and HSCRW50 compared to the plain concrete. The reduction in mass of the samples can be attributed to the relatively lower corrosion resistance of recycled ceramic waste aggregate in comparison with the natural coarse aggregate. Upon exposure to the acidic environment, the sample's surface started to deteriorate and dissolved in the acidic solution, which resulted in loss of mass of the specimen.

4.3.2.2. Compressive strength. The compression test was conducted on conditioned and unconditioned cubic samples to determine the strength retention of different mixtures after exposure to acidic environment. The sulfuric acid permeated through the voids and pores of the concrete and influenced the matrix and bond between

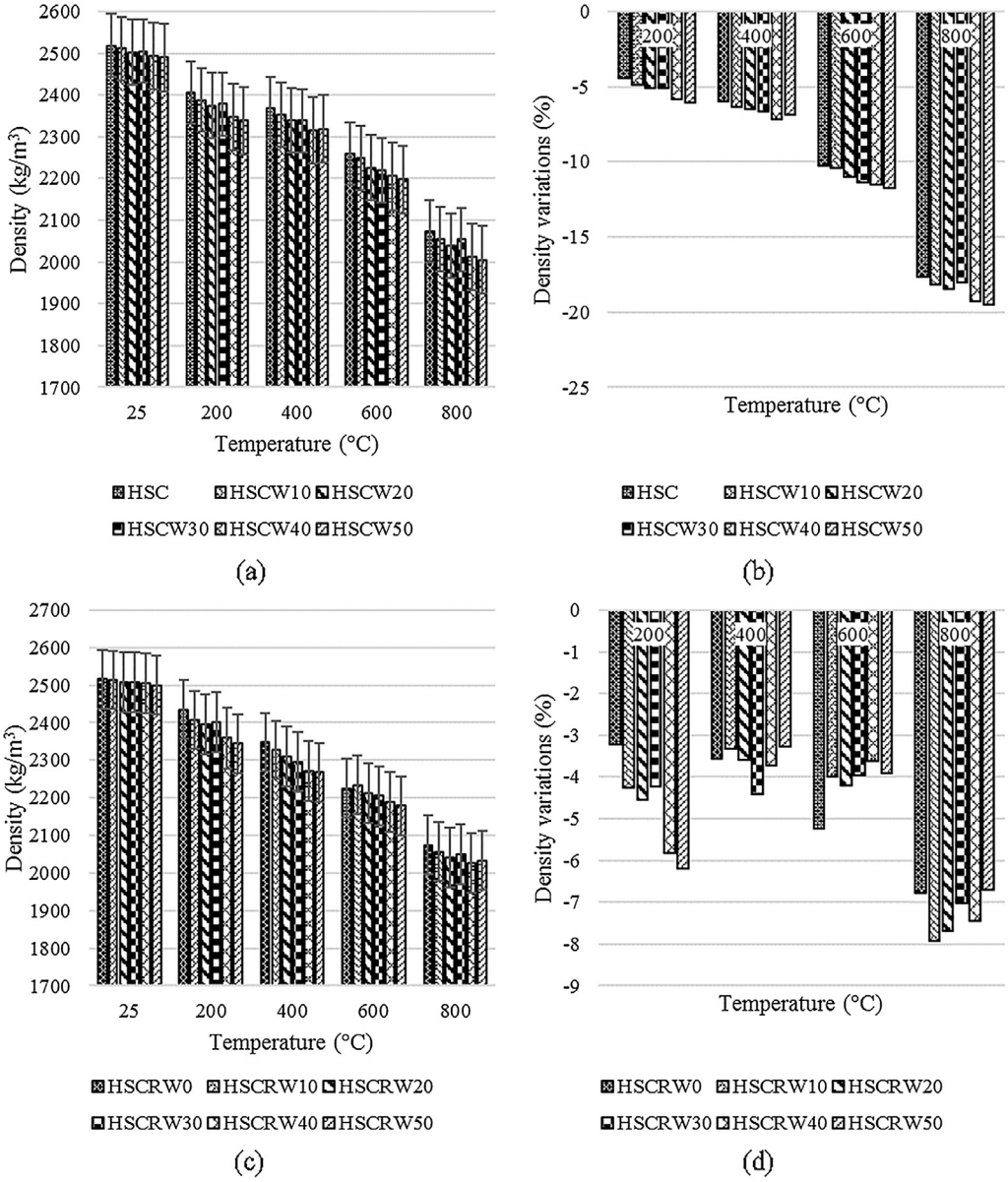

Fig. 28. Effects of elevated temperatures on concrete density: (a) Concrete density of HSCW mixtures, (b) Concrete density variations of HSCW mixtures, (c) Concrete density of HSCRW mixtures, (d) Concrete density variations of HSCRW mixtures.

concrete components, resulting in strength deterioration. Fig. 26(a) and (b) respectively show the compressive strength of HSCW and HSCRW concrete mixtures, while Fig. 26(c) and (d) illustrate the strength retentions. As seen, the highest resistance against acidic environment was observed for mixtures with 10% wollastonite content. According to the results, the compressive strength retention did not show a distinct trend with increasing values of wollastonite content. For example, HSCW10, HSCW20, HSCW40, and HSCW50 showed a strength retention of 96%, 91%, 93%, and 95%, respectively. Furthermore, the effects of acidic environment on strength deterioration of HSCRW mixtures was more pronounced, e.g., 11% strength reduction was observed in HSCRW50, respectively. This could be attributed to the lower resistance of recycled ceramic waste aggregate compared to the natural coarse aggregate.

4.3.3. Effects of elevated temperatures on concrete properties

The specimens were subjected to elevated temperatures of 200 °C, 400 °C, 600 °C, and 800 °C for one hour by using an electrical oven as shown in Fig. 27. After cooling down to the ambient temperature, the effects of the selected elevated temperatures on density and compressive strength of samples were evaluated.

4.3.3.1. Concrete density. Fig. 28(a) and (c) respectively show the effects of elevated temperatures on density of HSCW and HSCRW mixtures, while Fig. 28(b) and (d) show the density variations of the aforementioned mixtures. As seen, the concrete density decreased with increasing temperature. For example, the density of the control concrete was reduced by 7% and 18% at 400 °C and 800 °C, respectively. The effects of temperature on density were almost identical for HSCW and HSCRW concrete mixtures, i.e., the reduction percentages were approximately equal. The reduction in density owed to the fact that at higher temperatures, higher water evaporation occurred in the specimen and as a result, the weight of the sample decreased.

4.3.3.2. Compressive strength. The effects of elevated temperatures on compressive strength of HSCW and HSCRW concrete mixtures are illustrated in Fig. 29(a) and (c), respectively. In addition, the

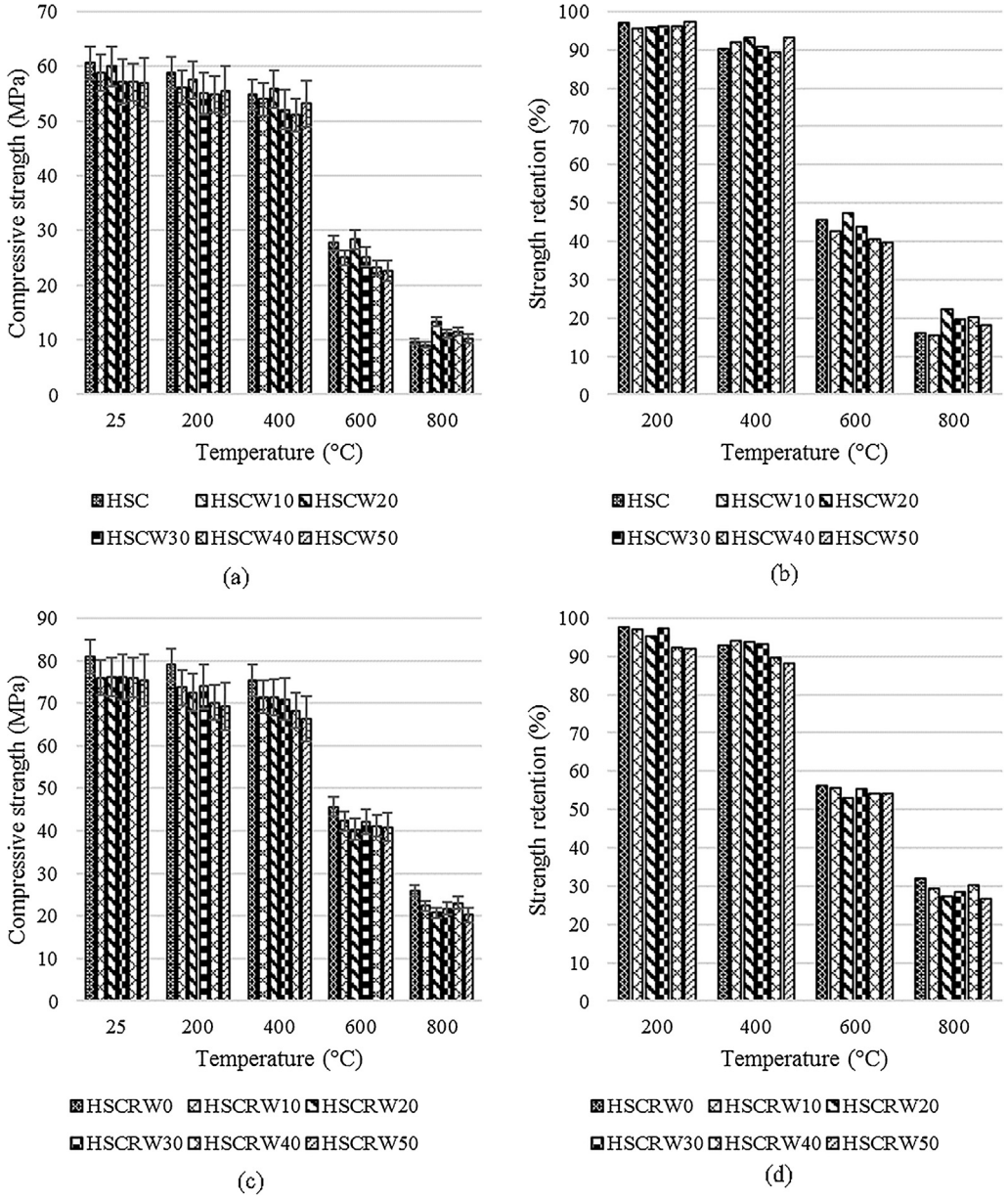

Fig. 29. Effects of elevated temperatures on compressive strength: (a) Compressive strength of HSCW mixtures, (b) Compressive strength variations of HSCW mixtures, (c) Compressive strength of HSCRW mixtures, (d) Compressive strength variations of HSCRW mixtures.

strength retention after exposure to elevated temperatures are depicted in Fig. 29(b) and (d) for HSCW and HSCRW mixtures, respectively. As observed, the compressive strength of concrete dropped as the temperature increased. For example, the compressive strength decreased by 44% and 68% in HSCRW0 at 600 °C and 800 °C, respectively. The strength reduction could be attributed to the fact that with increasing temperature, the moisture in the concrete turned into super-heated steam, causing the internal pressure to escalate. The pressure value can increase up to 8 to 10 MPa, which results in strength reduction due to crack formation. In addition, concrete is a complex material which consists of several components with different thermal coefficients. Therefore, the bond between the cement paste and aggregate diminishes at high temperatures, since they expand to different extents. Moreover, it was observed that wollastonite did not have a considerable effect on the compressive strength at elevated temperatures due to its inert nature [59]. Furthermore, the strength reduction was less pronounced in mixtures with recycled ceramic waste aggregate. For the sake of illustration, the compressive strength of HSCW10 and HSCRW10 dropped by 84% and 70% at 800 °C, respectively. This indicated that concrete with recycled ceramic waste aggregate performed better than the plain concrete when subjected to fire, since ceramic aggregate were more fire resistant compared to the natural coarse aggregate.

4.3.4. Ultrasonic pulse velocity

The ultrasonic pulse velocity test was performed on cubic samples to assess the quality and integrity of the hardened concrete per ASTM C597 [46]. For this purpose, three identical cubic samples were selected for each concrete mixture at the age of 28, 56, and 91 days and the velocity of ultrasonic wave passing through the specimen was calculated by using an Ultrasonic Concrete Tester110-240 V 50/60 Hz 1Ph device.

The UPV values and their variations for different concrete mixtures are presented in Fig. 30. In particular, Fig. 30(a) and Fig. 30(b) demonstrate the UPV values and their variations for HSCW mixtures. As seen, replacing cement with wollastonite particles slightly reduced the UPV value, for example, about 3% reduction occurred in HSCW50.

On the other hand, substitution of natural coarse aggregate with recycled ceramic waste, improved the integrity of concrete mixtures. For example, the UPV of HSCRW0 increased about 10%

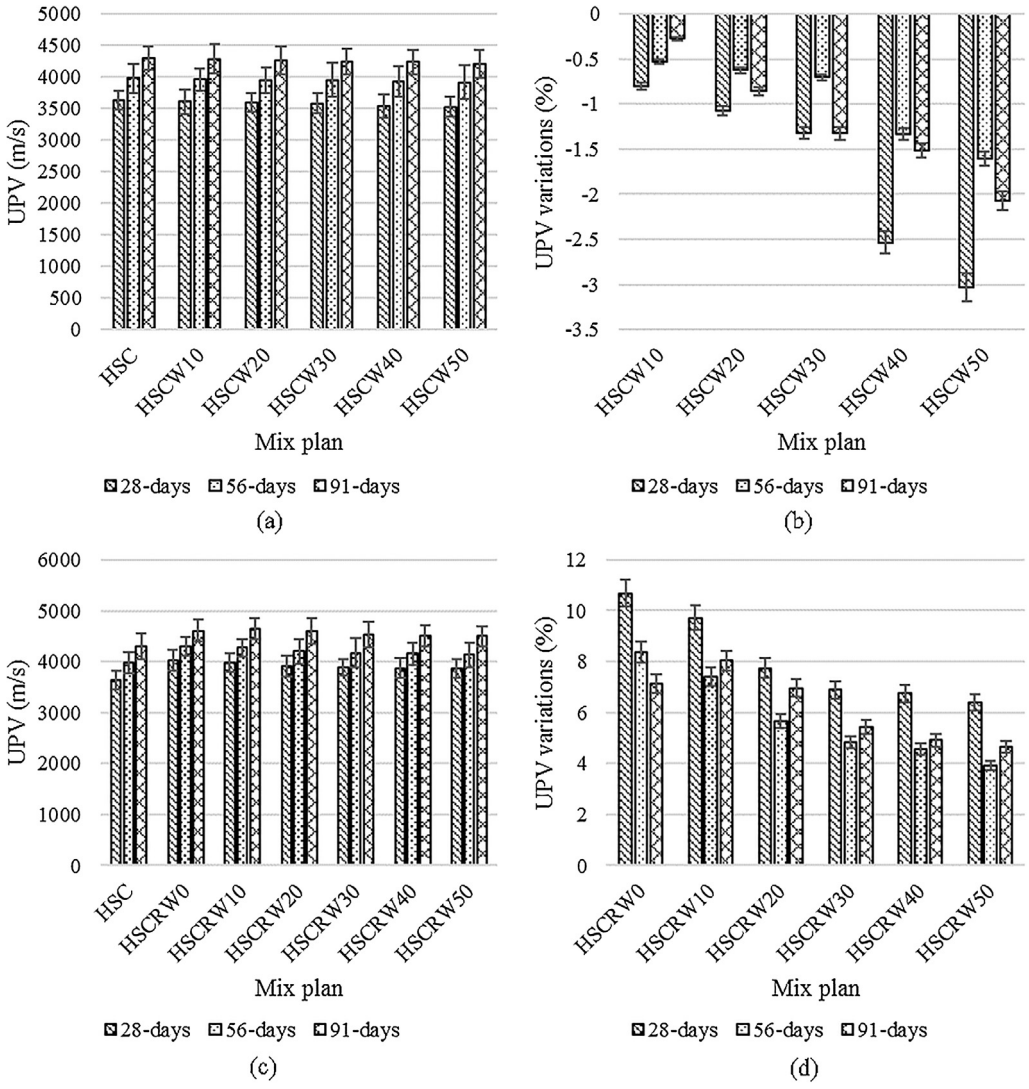

Fig. 30. UPV test results: (a) UPV of HSCW mixtures, (b) UPV variations of HSCW mixtures with respect to HSC, (c) UPV of HSCRW mixtures, (d) UPV variations of HSCRW mixtures with respect to HSC.

compared to the control concrete. This could be due to the pozzolanic reactions between ceramic waste aggregate and other components, which introduced more CSH gel into the concrete texture and reduced the voids and pores in the concrete.

4.4. Scanning electron microscopy (SEM) analysis

The morphology of different mixtures are presented in Fig. 31 (a)–(e). In particular, Fig. 31(a) shows the SEM image of the control

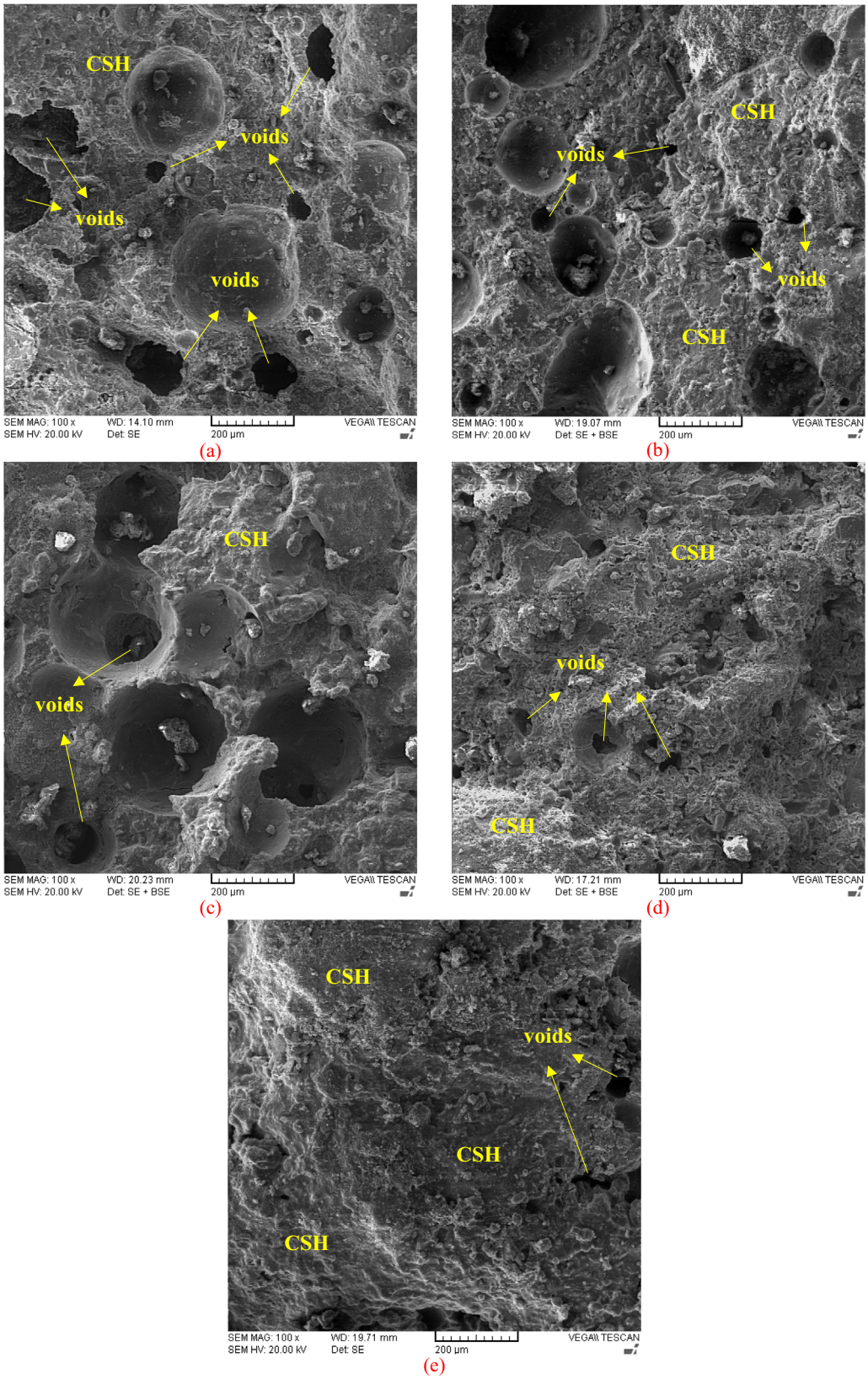

Fig. 31. SEM images of mixtures: (a) Control sample, (b) HSCW10, (c) HSCW50, (d) HSCRW10, (e) HSCRW50.

sample. With reference to this figure, several pores were observed in the concrete matrix which indicated insufficient hydration. Fig. 31(b) illustrates the microstructure of mixture HSCW10 in which 10% of cement was replaced with wollastonite particles. As seen, inclusions of wollastonite particles led to a denser matrix with fewer voids due to micro-filling effect of these particles. By increasing the wollastonite content in the mixture, a higher pore refinement was achieved as shown in Fig. 31(d). As observed, concrete with 50% wollastonite content exhibited a less porous structure in comparison with the previous figure. Furthermore, Fig. 31 (d) and (e) illustrate the micrograph images of mixtures HSCRW10 and HSCRW50, respectively. According to these figures, replacing half of the natural coarse aggregate with ceramic waste aggregate improved the pore structure of concrete. As seen, there was a noticeable increase in the amount of CSH gel which could be attributed to the pozzolanic reaction between ceramic waste aggregate and portlandite as reported by previous studies [27,47,48]. In addition, it can be inferred from comparing Fig. 31(d) and (e) that the micro-filling effect of wollastonite particles further reduced the pore size and resulted in a denser structure in HSCRW50 compared to HSCRW10.

4.5. Optimum wollastonite percentage

This paper investigated the utilization of wollastonite particles and recycled ceramic waste aggregate in high strength concrete. Based on the experiment results, the concrete quality in terms of workability and compressive strength degraded with increasing wollastonite content; however, splitting tensile and flexural strength and durability properties such as water absorption were enhanced. Therefore, the optimum percentage of wollastonite particles to be utilized as partial replacement of cement in high strength concrete production was indicated to be 30%. This was in agreement with the previous studies, which investigated the combined utilization of wollastonite and other alternative materials in concrete. Kalla et al. [34] evaluated the properties of concrete containing 5%, 10%, and 15% wollastonite as partial replacement of cement and showed that incorporating 10% to 15% wollastonite led to the highest compressive and tensile strength. In another study, wollastonite and fly ash were utilized in concrete mixtures to replace cement in different dosages and it was shown that replacing 10–15% of cement with wollastonite together with 40% of fly ash led to the best compressive and tensile strength in concrete [16]. Similarly, Dey et al. [33] showed that replacing 10% of cement with wollastonite improved the flexural strength of concrete. Soliman and Nehdi [36] replaced 4% and 12% of cement with wollastonite and concluded that higher dosage of wollastonite resulted in higher crack resistance and lower shrinkage. Fig. 32 shows the optimum wollastonite percentages for concrete production recommended by different studies.

In summary, using wollastonite particles as partial replacement of cement would reduce the amount of greenhouse gas emissions due to Portland cement production. Furthermore, replacing natural coarse aggregate with ceramic waste aggregate would help addressing the problems associated with its disposal. Ceramic waste is one the most common waste materials in Iran since it is one the major building materials in construction industry. Therefore, using it in concrete production would reduce the demand of landfill space. Besides, as shown in this study, partial replacement of natural coarse aggregate with ceramic waste aggregate increased the strength and durability of the concrete.

5. Conclusions

Based on the results, the following conclusions were drawn:

1- The workability of concrete decreased with increasing wollastonite content. Furthermore, partial substitution of natural coarse aggregate with ceramic waste aggregate further reduced the workability.
2- Combined utilization of wollastonite particles and ceramic waste aggregate reduced the fresh density of concrete; however, the maximum reduction was below 1%. The slight reduction in fresh density was due to the relatively lower density of wollastonite particles compared to that of cement.
3- Concrete specimens with wollastonite particles showed reduced compressive strength compared to the control sample. On the other hand, concrete with recycled ceramic waste aggregate exhibited 34% higher compressive strength at curing age of 28 days with respect to the control concrete.
4- Inclusions of wollastonite particles enhanced the splitting tensile strength, flexural strength, and modulus of elasticity of concrete. At 50% replacement ratio, the aforementioned properties were increased by 24%, 10%, and 4% compared to the control sample, respectively. Moreover, incorporating ceramic waste aggregate contributed to the aforementioned

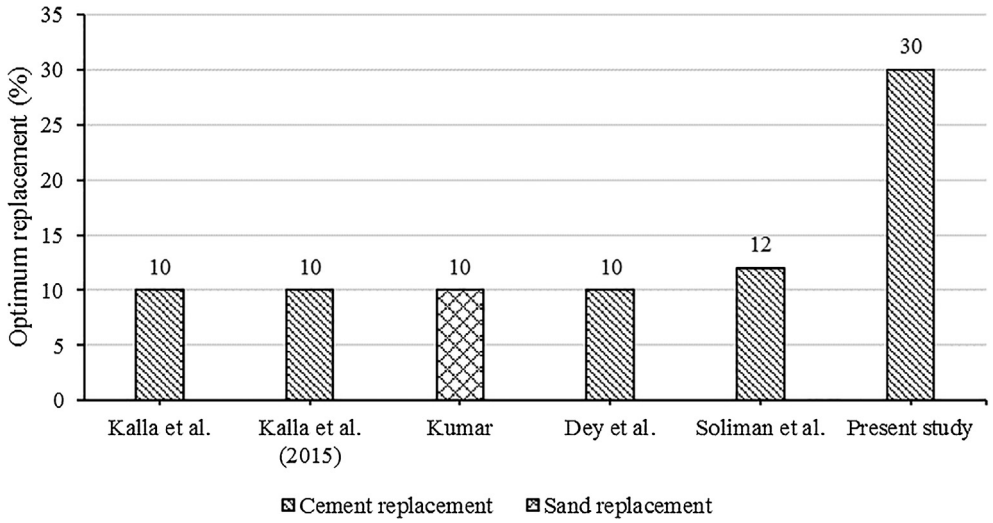

Fig. 32. Optimum wollastonite percentage recommended by different studies.

properties which was attributed to enhanced interlocking between aggregates and cement paste and pozzolanic reaction between ceramic waste aggregate and portlandite.

5- The water absorption of concrete specimens decreased with increasing wollastonite content. This owed to the filling effect of wollastonite particles, which led to pore refinement in concrete matrix.

6- Due to lower permeability and absorptivity of concrete containing wollastonite and ceramic waste aggregate, HSCW mixtures showed higher strength retention after exposure to acidic environment with reference to the control concrete. However, the strength retention of HSCRW mixtures was slightly lower than that of the control concrete due to lower corrosion resistance of ceramic waste aggregate compared to natural coarse aggregate.

7- The density and compressive strength of concrete were significantly reduced at elevated temperatures. Up to 80% reduction in compressive strength was observed at 800 °C, which was attributed to the increase in internal pressure of specimens and formation of surface cracks. Concrete with recycled ceramic waste aggregate performed better under fire since ceramic aggregate were more fire resistant compared to the natural coarse aggregate.

8- The results of UPV test showed that utilization of ceramic waste aggregate as partial replacement of natural coarse aggregate improved the integrity and pore structure of the concrete. Furthermore, the inclusions of wollastonite particles resulted in a slight reduction in UPV values, which could be due to lower quality of the interfacial transition zone (ITZ) of concrete with wollastonite.

Conflict of interest

None declared.

Acknowledgement

Authors would like to gratefully acknowledge the staff at the Concrete Laboratory of Civil Engineering Department at Isfahan (Khorasgan) Branch, Islamic Azad University, and also Shahrekord cement plant for their support during this research.

Funding

This research did not receive any specific grant from funding agencies in the public, commercial, or not-for-profit sectors.

References

[1] A.M. Rashad, A preliminary study on the effect of fine aggregate replacement with metakaolin on strength and abrasion resistance of concrete, Constr. Build. Mater. 44 (2013) 487–495, https://doi.org/10.1016/j.conbuildmat.2013.03.038.

[2] D.N. Huntzinger, T.D. Eatmon, A life-cycle assessment of Portland cement manufacturing: comparing the traditional process with alternative technologies, J. Clean. Prod. 17 (2009) 668–675, https://doi.org/10.1016/j.jclepro.2008.04.007.

[3] P.K. Mehta, H. Meryman, Tools for reducing carbon emissions due to cement consumption, Structure. 1 (2009) 11–15.

[4] D.J.M. Flower, J.G. Sanjayan, Green house gas emissions due to concrete manufacture, Int. J. Life Cycle Assess. 12 (2007) 282–288, https://doi.org/10.1007/s11367-007-0327-3.

[5] A.M. Rashad, D.M. Sadek, H.A. Hassan, An investigation on blast-furnace stag as fine aggregate in alkali-activated slag mortars subjected to elevated temperatures, J. Clean. Prod. 112 (2016) 1086–1096, https://doi.org/10.1016/j.jclepro.2015.07.127.

[6] İ. Yüksel, T. Bilir, Ö. Özkan, Durability of concrete incorporating non-ground blast furnace slag and bottom ash as fine aggregate, Build. Environ. 42 (2007) 2651–2659.

[7] S.T. Ramesh, R. Gandhimathi, P.V. Nidheesh, S. Rajakumar, S. Prateepkumar, Use of furnace slag and welding slag as replacement for sand in concrete, Int. J. Energy Environ. Eng. 4 (2013) 3, https://doi.org/10.1186/2251-6832-4-3.

[8] E. Crossin, The greenhouse gas implications of using ground granulated blast furnace slag as a cement substitute, J. Clean. Prod. 95 (2015) 101–108, https://doi.org/10.1016/j.jclepro.2015.02.082.

[9] A. Gholampour, T. Ozbakkaloglu, Performance of sustainable concretes containing very high volume Class-F fly ash and ground granulated blast furnace slag, J. Clean. Prod. 162 (2017) 1407–1417, https://doi.org/10.1016/j.jclepro.2017.06.087.

[10] P.H. Shih, Z.Z. Wu, H.L. Chiang, Characteristics of bricks made from waste steel slag, Waste Manage. 24 (2004) 1043–1047, https://doi.org/10.1016/j.wasman.2004.08.006.

[11] V.S. Devi, B.K. Gnanavel, Properties of concrete manufactured using steel slag, Procedia Eng. 97 (2014) 95–104.

[12] P. Shoaei, S. Zolfaghary, N. Jafari, M. Dehestani, M. Hejazi, Investigation of adding cement kiln dust (CKD) in ordinary and lightweight concrete, Adv. Concr. Constr. 5 (2017), https://doi.org/10.12989/acc.2017.5.2.101.

[13] S.A. Zareei, F. Ameri, F. Dorostkar, S. Shiran, Partial replacement of limestone and silica powder as a substitution of cement in lightweight aggregate concrete, Civ. Eng. J. 3 (2017) 727–740.

[14] S.A. Zareei, F. Ameri, N. Bahrami, Microstructure, strength, and durability of eco-friendly concretes containing sugarcane bagasse ash, Constr. Build. Mater. 184 (2018) 258–268.

[15] A. Bahurudeen, D. Kanraj, V. Gokul Dev, M. Santhanam, Performance evaluation of sugarcane bagasse ash blended cement in concrete, Cem. Concr. Compos. 59 (2015) 77–88, https://doi.org/10.1016/j.cemconcomp.2015.03.004.

[16] P. Kalla, A. Misra, R.C. Gupta, L. Csetenyi, V. Gahlot, A. Arora, Mechanical and durability studies on concrete containing wollastonite-fly ash combination, Constr. Build. Mater. 40 (2013) 1142–1150.

[17] N. Tošić, S. Marinković, N. Pecić, I. Ignjatović, J. Dragaš, Long-term behaviour of reinforced beams made with natural or recycled aggregate concrete and high-volume fly ash concrete, Constr. Build. Mater. 176 (2018) 344–358.

[18] H. Mohammadhosseini, A.S.M. Abdul Awal, J.B. Mohd, Yatim, The impact resistance and mechanical properties of concrete reinforced with waste polypropylene carpet fibres, Constr. Build. Mater. 143 (2017) 147–157, https://doi.org/10.1016/j.conbuildmat.2017.03.109.

[19] D.-Y. Yoo, N. Banthia, J.-M. Yang, Y.-S. Yoon, Size effect in normal-and high-strength amorphous metallic and steel fiber reinforced concrete beams, Constr. Build. Mater. 121 (2016) 676–685.

[20] V. Afroughsabet, T. Ozbakkaloglu, Mechanical and durability properties of high-strength concrete containing steel and polypropylene fibers, Constr. Build. Mater. 94 (2015) 73–82.

[21] A. Dehghan, K. Peterson, A. Shvarzman, Recycled glass fiber reinforced polymer additions to Portland cement concrete, Constr. Build. Mater. 146 (2017) 238–250.

[22] A.B. Kizilkanat, N. Kabay, V. Akyüncü, S. Chowdhury, A.H. Akça, Mechanical properties and fracture behavior of basalt and glass fiber reinforced concrete: an experimental study, Constr. Build. Mater. 100 (2015) 218–224.

[23] A.S.M.A. Awal, H. Mohammadhosseini, Green concrete production incorporating waste carpet fiber and palm oil fuel ash, J. Clean. Prod. 137 (2016) 157–166, https://doi.org/10.1016/j.jclepro.2016.06.162.

[24] O. Zimbili, W. Salim, M. Ndambuki, A review on the usage of ceramic wastes in concrete production, Int. J. Civil, Environ. Struct. Constr. Archit. Eng. 8 (2014) 91–95.

[25] K. Rahal, Mechanical properties of concrete with recycled coarse aggregate, Build. Environ. 42 (2007) 407–415.

[26] D.J. Anderson, S.T. Smith, F.T.K. Au, Mechanical properties of concrete utilising waste ceramic as coarse aggregate, Constr. Build. Mater. 117 (2016) 20–28, https://doi.org/10.1016/j.conbuildmat.2016.04.153.

[27] K. Rashid, A. Razzaq, M. Ahmad, T. Rashid, S. Tariq, Experimental and analytical selection of sustainable recycled concrete with ceramic waste aggregate, Constr. Build. Mater. 154 (2017) 829–840.

[28] D.J. Martins, J.R. Correia, J. de Brito, The effect of high temperature on the residual mechanical performance of concrete made with recycled ceramic coarse aggregates, Fire Mater. 40 (2016) 289–304.

[29] J.P.B. Vieira, J.R. Correia, J. De Brito, Post-fire residual mechanical properties of concrete made with recycled concrete coarse aggregates, Cem. Concr. Res. 41 (2011) 533–541.

[30] D. Ren, C. Yan, P. Duan, Z. Zhang, L. Li, Z. Yan, Durability performances of wollastonite, tremolite and basalt fiber-reinforced metakaolin geopolymer composites under sulfate and chloride attack, Constr. Build. Mater. 134 (2017) 56–66.

[31] H. Naderpour, M. Mirrashid, Compressive strength of mortars admixed with wollastonite and microsilica, Mater. Sci. Forum, Trans. Tech. Publ. (2017) 415–418.

[32] M.A. Wahab, I.A. Latif, M. Kohail, A. Almasry, The use of Wollastonite to enhance the mechanical properties of mortar mixes, Constr. Build. Mater. 152 (2017) 304–309.

[33] V. Dey, R. Kachala, A. Bonakdar, B. Mobasher, Mechanical properties of micro and sub-micron wollastonite fibers in cementitious composites, Constr. Build. Mater. 82 (2015) 351–359.

[34] P. Kalla, A. Rana, Y.B. Chad, A. Misra, L. Csetenyi, Durability studies on concrete containing wollastonite, J. Clean. Prod. 87 (2015) 726–734.

[35] M.A. Minoux, Cendres volantes et microcendres: procédés d'obtention. Conséquences physiques et chimiques sur le système microcendres-ciments-eau, 1994.

[36] A.M. Soliman, M.L. Nehdi, Effects of shrinkage reducing admixture and wollastonite microfiber on early-age behavior of ultra-high performance concrete, Cem. Concr. Compos. 46 (2014) 81–89.
[37] S. Kwon, T. Nishiwaki, H. Choi, H. Mihashi, Effect of wollastonite microfiber on ultra-high-performance fiber-reinforced cement-based composites based on application of multi-scale fiber-reinforcement system, J. Adv. Concr. Technol. 13 (2015) 332–344.
[38] ASTM C192/C192M-16, Standard Practice for Making and Curing Concrete Test Specimens in the Laboratory, in: ASTM International West Conshohocken, PA, 2016.
[39] ASTM C143/C143M-15a, Standard Test Method for Slump of Hydraulic-Cement Concrete, in: ASTM International West Conshohocken, PA, 2015.
[40] ASTM C138/C138M-14, Standard Test Method for Density (Unit Weight), Yield, and Air Content (Gravimetric) of Concrete., in: ASTM International, West Conshohocken, PA, 2014.
[41] ASTM C39/C39M-16, Standard Test Method for Compressive Strength of Cylindrical Concrete Specimens, in: ASTM International West Conshohocken, PA, 2016.
[42] ASTM C496/C496M-17, Standard Test Method for Splitting Tensile Strength of Cylindrical Concrete Specimens, in: ASTM International West Conshohocken, PA, 2017.
[43] ASTM C78/C78M-16, Standard Test Method for Flexural Strength of Concrete (Using Simple Beam with Third-Point Loading), in: ASTM International West Conshohocken, PA, 2016.
[44] ASTM C469/C469M-14, Standard Test Method for Static Modulus of Elasticity and Poisson's Ratio of Concrete in Compression, in: ASTM International West Conshohocken, PA, 2014.
[45] ASTM C642-13, Standard Test Method for Density, Absorption, and Voids in Hardened Concrete. American Society for Testing and Materials, in: ASTM International, West Conshohocken, PA, 2013.
[46] ASTM C597-16, Standard Test Method for Pulse Velocity Through Concrete, in: ASTM International West Conshohocken, PA, 2016.
[47] C. Medina, M.I.S. de Rojas, M. Frías, Freeze-thaw durability of recycled concrete containing ceramic aggregate, J. Clean. Prod. 40 (2013) 151–160.
[48] C. Medina, M. Frías, M.I.S. De Rojas, Microstructure and properties of recycled concretes using ceramic sanitary ware industry waste as coarse aggregate, Constr. Build. Mater. 31 (2012) 112–118.
[49] H. Higashiyama, F. Yagishita, M. Sano, O. Takahashi, Compressive strength and resistance to chloride penetration of mortars using ceramic waste as fine aggregate, Constr. Build. Mater. 26 (2012) 96–101.
[50] R. Mathur, A.K. Mishra, P. Goel, Marble slurry dust and wollastonite-inert mineral admixture for cement concrete, 2007.
[51] ACI Committee 318, Building Code Requirements for Structural Concrete (ACI 318-14) and Commentary (ACI 318R-14), in: American Concrete Institute, Farmington Hills, MI, 2014.
[52] CSA, Design of Concrete Structures, Can. Stand. Assoc., 2004.
[53] EC-04, B.S. Institution, Eurocode 2: Design of Concrete Structures: Part 1-1: General Rules and Rules for Buildings, 2004.
[54] J.S.C.E, Engineers, Standard Specification for Concrete Structure, 2007.
[55] J.C.I, Guidelines for Control of Cracking of Mass Concrete, Japan Concr. Inst., 2008.
[56] NZ, Concrete Structures Standard: NZS 3101, 2006.
[57] Management and planning organization of I.R. Iran, Iranian code of practice, ABA, 2001.
[58] G.D. Ransinchung, B. Kumar, V. Kumar, Assessment of water absorption and chloride ion penetration of pavement quality concrete admixed with wollastonite and microsilica, Constr. Build. Mater. 23 (2009) 1168–1177.
[59] X. Gao, A. Zhang, S. Li, B. Sun, L. Zhang, The resistance to high temperature of magnesia phosphate cement paste containing wollastonite, Mater. Struct. 49 (2016) 3423–3434.